2010

Exploration of Monostrand Use in Segmental Box Girder Bridges

Herbert Houston Spear

THE FLORIDA STATE UNIVERSITY

COLLEGE OF ENGINEERING

EXPLORATION OF MONOSTRAND USE IN SEGMENTAL BOX GIRDER BRIDGES

By

H. HOUSTON SPEAR

A Thesis submitted to the
Department of Civil and Environmental Engineering
in partial fulfillment of the
requirements for the degree of
Master of Science

Degree Awarded:
Spring Semester, 2010

The members of the committee approve the thesis of H. Houston Spear defended on April 2, 2010.

_____
Michelle Rambo-Roddenberry
Professor Directing Thesis

_____
Lisa Spainhour
Committee Member

_____
Kamal Tawfiq
Committee Member

Approved:

_____
Kamal Tawfiq, Chair, Department of Civil and Environmental Engineering

The Graduate School has verified and approved the above-named committee members.

For Herb, Bertha, and Matt

ACKNOWLEDGEMENTS

I would first like to thank Dr. Michelle Rambo-Roddenberry, P.E. for the wisdom and guidance she imparted. Her efforts and her friendship have made writing this thesis a truly enjoyable experience. I would also like to thank Dr. Lisa Spainhour, P.E. and Dr. Kamal Tawfiq, P.E. for being on my graduate committee and being willing to assist me in the creation of this thesis. I would like to recognize Dr. Juan Jose Goni, P.E. for his vision and his work on the Metrorrey viaduct, which provided the starting point for this research. I would also like to thank the Florida Department of Transportation for funding this project and Marc Ansley, P.E. for his input. My thanks also go out to the entire faculty and staff at the Department of Civil and Environmental Engineering at FSU for giving me the tools and the confidence to undertake this project.

I would like to thank my parents, Herb and Bertha, and my brother Matt for their unconditional love and support. The sacrifices they have made to encourage my college career have been too numerous to count and not one has been forgotten.

I would also like to extend special thanks to Melody Lovin and my friends Jon Chipperfield and Nick Bouchard for the assistance and motivation they have given me so that I could achieve my goal of obtaining a Master's degree. And also to John Cornelius of SWPC for giving me his time and information so readily when so many others could not.

DISCLAIMER

The information contained within this thesis, referenced design plans and calculations are for educational purposes only and are not intended as a final design or for construction. The plan views, cross sections, and computer outputs labeled as dead and live loads are used only as a reference and theoretical examples. The ideas and opinions expressed here are those of the author and are not necessarily associated with the goals or plans of any agency or entity.

TABLE OF CONTENTS

LIST OF TABLES

LIST OF FIGURES

LIST OF SYMBOLS

A	Cross-sectional area
A_s	Cross-sectional area of steel reinforcing
A_{vf}	Cross-sectional area of steel reinforcing resisting frictional shear
b	Base, horizontal dimension of an object
c	Distance from neutral axis to outer compressive fiber
d	Depth, vertical dimension of an object
E	Young's Modulus of Elasticity
e	Base of Natural logs
f'_c	Compressive strength of concrete
f_{max}	Maximum bending stress in outer fibers
f_{ult}	Ultimate force that can be provided by a single monostrand
f_y	Yield strength of steel reinforcement
I	Moment of Inertia for an individual, simple shape
I_x	Moment of Inertia for an entire cross section
K	Wobble coefficient, representing unintended deviation in tendon layout
L	Total length of a segment subjected to elongation
l_{px}	Distance along tendon from jacking end to point of interest
M	External bending moment
m	Mass of an object
P	Post-Tensioning force acting on a cross-section
P_{px}	Force in Post-Tensioning tendons at the location of interest
P_{pj}	Force in Post-Tensioning tendon at the point of jacking

P_{strand}	Web monostrand force after all losses
Q	First moment of area
r	Radius of gyration
s	Spacing, center-to-center of monostrand or steel reinforcement
t_{web}	web thickness at location of interest
V_c	Nominal shear strength provided by concrete
V_n	Nominal shear stress
y	Distance from the centroid of an object to the neutral axis
α_{px}	Angular change of tendon profile from jacking end to point of interest
δ	Elongation, in this instance, elongation of a monostrand
σ	Normal stress
$\sigma_{1,3}$	Major and minor principal stresses, respectively
$\sigma_{x,y}$	Normal stresses (compression and tension) acting on an element
$\sigma_{y(strand)}$	Normal stress as a result of web monostrand
$\tau_{x,y}$	Shear forces acting on an element
μ	frictional coefficient
μ_p	Post-Tensioning frictional coefficient
v	Shear stress

LIST OF ABBREVIATIONS

AASHTO	American Association of State Highway and Transportation Officials
ACI	The American Concrete Institute
DSI	DYWIDAG-SYSTEMS INTERNATIONAL
FDOT	Florida Department of Transportation
ft	Foot or feet
HDPE	High-density polyethylene, a common petroleum derived thermoplastic
in.	Inch or inches
ksf	Kips per square foot
ksi	Kips per square inch
lb	Pound(s)
LRFD	Load and Resistance Factor Design
PP	Polypropylene, medium density thermoplastic
psi	Pounds per square inch
PT	Post-Tensioning
PTI	Post-Tensioning Institute
s.f., sf	Square foot
SWPC	Sumiden Wire Products Corporation
yd^3	Cubic yard(s)

ABSTRACT

For the past several decades the segmental box girder bridge has proven itself to be one of the more efficient bridge types. Using reusable form work, segments are match-cast, ensuring a more perfect connection during the construction phase. These benefits in conjunction with the fact that the costs of startup and form work are absorbed into the total cost of each segment mean that the longer the final bridge is, the less the cost is per segment, making the segmental box girder bridge one of the most popular long bridge types constructed in the U.S.

To minimize cost, it is important to design each segment for efficiency in terms of quantity of longitudinal and transverse post-tensioning and reinforcing steel. The inclusion of post-tensioning technology results in an overall compressive state in the longitudinal and transverse directions of the segments, improving structure strength and service life. However, despite the benefits inherent in using post-tensioning technology, the webs still contain standard deformed reinforcement. The goal of this research is to fit a greased and sheathed monostrand within a segment in a way that both webs and bottom flange would be placed in a state of compression, thereby reducing the demand for standard web reinforcement and, hopefully, segment cost. The research objectives include analyzing principal stresses in the webs of the segment, modifying the segment so as to restrain the monostrand within the webs, designing any additional reinforcement that may be necessary, and finally comparing the estimated construction cost of the new design with that of a pre-existing structure.

The results from this research have shown that it is indeed possible to place a greased and sheathed monostrand within the webs of a segment with beneficial results and that the demand for standard deformed reinforcement will thus be reduced.

CHAPTER 1

INTRODUCTION

1.1 Overview

The strength of concrete mirrors that of its composite parts; stones and mortars are thought of immediately by most as being durable under pressure. Under compression, concrete can easily exhibit strengths of 4000 psi or more. However, when placed in tension, concretes, mortars, and even natural stones rapidly fail. This inherent weakness displayed by this building material limited its uses until the second half of the 19th century.

Within this era, deformed steel rebar were introduced into the tensile regions of concrete structures such as beams, greatly increasing their carrying capacity and reducing their cross sections. This new *reinforced concrete* allowed a wide range of new structures to be built, from bridges to dams, and more. Reinforced concrete, however, had its own drawbacks. The property of the steel rebar to strain much more so than the surrounding concrete would lead to the formation of cracks in the member. Over time moisture would enter these cracks and corrode the rebar, reducing structure service life.

The next great advancement in the realm of concrete design was pre- and post-tensioning. Once strong enough steel materials were developed, designers realized that they could put high-strength steel strands in tension and then release those tensile forces onto the surrounding concrete member. Doing so placed the normally tensile region of the concrete member under a compressive force. It would now take a much greater tensile force to cause cracking in a structure with identical cross-sectional area than in a cross section with only standard rebar reinforcement. The strands can be tensioned before the concrete is cast (pretensioning) or after the concrete is cast (post-tensioning).

For a little over a half-century, pre- and post-tensioning has allowed more durable and efficient concrete structures to be built than had ever been possible in the 9,000 year history[1] of

[1] **.** (p.1) *9,000 year history:* Refers to the discovery of concrete floor slabs in the ancient settlement of Yiftahel, Israel. Even though this time frame predates the invention of pottery Neolithic kilns were capable of the 900° required to calcine limestone. 1 inch cube samples of the floor slabs at Yiftahel produced up to 6500 psi in lab tests. Lime mortars from Greece, however, can be as old as 12,000 B.C.

concrete. Since the introduction of pre- and post-tensioning, the industry has seen more and more efficient structures exhibiting reduced cross-sectional areas and more efficient layouts of tensile reinforcements. Arguably, one of the most efficient structures ever to be developed from this march toward greater capacity while reducing costs is the segmental box girder bridge.

Segmental box girder bridges are some of the most efficient structures in terms of their support capacity-to-material use ratio. Their efficiency stems from the blending of high-strength prestressing strands transversely in the deck and post-tensioning strands that longitudinally join sections together. This combination of reinforcing schemes allows a transverse deck supporting several lanes of live traffic to be held together in permanent compression and still deliver the necessary strength and longevity demanded from the most important of bridges.

While pre- and post-tensioned strands are used extensively for transverse and longitudinal reinforcement -- typically in the form of multi-strand tendons -- standard reinforcement is still used within the box section of the girder. By replacing the standard reinforcement in the webs with post-tensioned monostrands, designers could potentially reduce construction and material costs while increasing service life. A monostrand is a single strand encased in a duct, as explained in Section 2.2.

1.2 Objective of Study

The goal of this research was to demonstrate the practicality of using greased and sheathed monostrands to enhance the shear capacity of the webs in typical segmental box girder bridges built by the span-by-span method of construction. The feasibility of the concept and the additional work that would be required for full implementation were determined as well.

The specific objectives of this study were as follows:

- To investigate the ability of monostrand to retain strength under tight curves
- To create a strand pattern within a typical segmental box girder section
- To quantify the resulting forces that occur after strand stressing
- To adjust the typical box girder design to accommodate the new forces
- To compare the new segmental box girder design with the old in terms of service, cost savings, and constructability

1.3 Scope of Study

The models and calculations featured in this research were based on a previously-designed bridge; in particular, the Choctawhatchee (Mid-Bay) Bridge in Florida, designed by Figg Bridge Engineers, Inc. in the 1990s, will often be referenced. The research focused on adjusting an existing bridge design with the addition of monostrand to the webs and then comparing the existing structure to the new design for efficiency and ease of construction. Although this research was based on the analysis of one bridge, the success of this project may mean cost savings on future segmental box girder bridge designs.

1.4 Significance of Study

As a result of this research the following benefits will be possible:

- Reduction of material use and construction costs for segmental box girder bridges
- Increase in structural life by placing every portion of the segment in compression

1.4.1 Reduction of Costs. By replacing standard web rebar with post-tensioned strands, an additional compressive force developed by the strands will be imparted to the web. Because this compressive force acts along the axis of each web, the box girder will resist a greater amount of shear than when using standard, un-stressed rebar.

1.4.2 Improved Structural Life. Another benefit of using post-tensioned monostrands in webs is that every section of the segment will be in compression in two directions. By placing the structure in compression, the occurrence of cracking and the infiltration of moisture within said cracks will be reduced. Greased and sheathed monostrands are encased in a sheath and protected from outside moisture.

1.5 Thesis Organization

This thesis is composed of four major chapters, after the introductory chapter. Chapter 2 discusses the literature reviews pertinent to the research. Chapter 3 discusses the methodology followed and the calculations involved in bringing this research to fruition. The fourth chapter

centers on the results of the methods in Chapter 3. The final chapter discusses the results of the research. Conclusions based on the research are also presented in this chapter, along with suggestions for future investigation into this subject.

CHAPTER 2

LITERATURE REVIEW

This chapter discusses current literature that supports the feasibility of implementing this technology into currently used segmental box girder bridge designs. The following topics were explored:

- Basics of Post-Tensioning
- Greased and Sheathed Monostrand
- Typical Segmental Box Girder Bridges
- The Metrorrey Viaduct
- Strength Loss from Bending

2.1 Basics of Post-Tensioning

Post-tensioning a structural concrete member means using prestressing strands to permanently compress the material, so that its ability to support a load is increased. For example, in a simply-supported beam subjected to gravity loads, the top of the beam is in compression while the bottom is in tension. To overcome concrete's weakness in tension, prestressing strands are placed in the beam near the bottom and are stressed; a compressive force is imparted into the beam by the anchorages at the ends of the strands. Post-tensioning strands are encased in ducts, not bonded with the concrete; "post" implies that the strands are tensioned after the concrete has cured. Multiple strands can be placed in a duct to make a tendon, or single strands (monostrands) can be used.

The details of a monostrand post-tensioning system are shown in Figure 2.1. The monostrand is composed of six steel wires helically wound around a seventh steel wire running down the middle of the strand. The wire is pulled through a duct, embedded in the concrete, and then through an anchor, also embedded in the concrete. The wire is then stressed to a pre-determined level. When the required amount of force is developed in the strand, the jack applying the force is removed, and the wedges inside the anchor transfer the strand forces to the surrounding concrete. This method concentrates the strand forces at the anchorages instead of transferring

the strand forces to the concrete along the length of the strand, as is the case with "pre-", as opposed to post-, tensioning using bonded strands. Pocket formers are used during concrete placement to create a void over the strand end so that the hydraulic jack may be attached to the strand. After stressing, for some applications, grease and sheathing are used to provide a lubricated channel for the strand (i.e., a "greased and sheathed monostrand"). Otherwise, grout is pumped into the remaining void between the strand and duct. This research focused on the use of unbonded, post-tensioned, greased and sheathed monostrands.

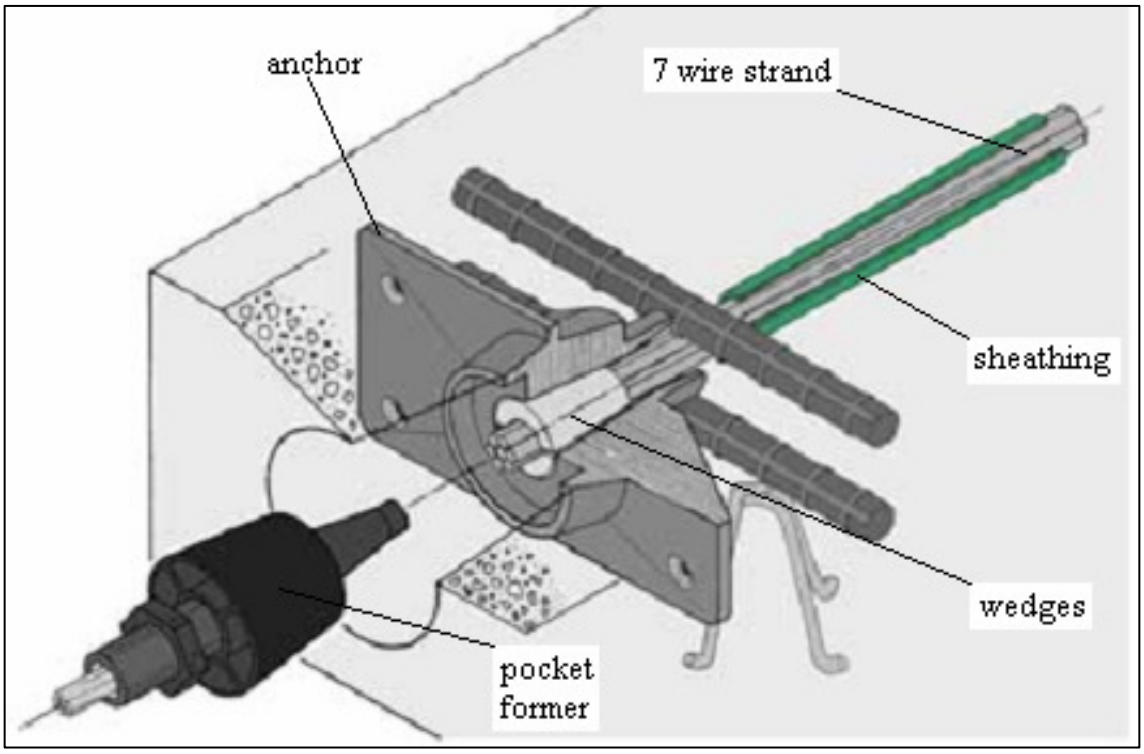

Figure 2.1 Post-Tensioned Monostrand Details (Specialty Steel 2010)

For the principles of post-tensioning to be applied to this research, certain specialized equations and equipment were considered. AASHTO LRFD Equation 5.9.5.2.2b-1 (Eqn. 2-1) determines the stress along any point of the strand:

$$P_{Px} = P_{Pj} e^{-(K\ell_{Px} + \mu_P \alpha_{Px})} \tag{2-1}$$

where P_{pj} is the force applied at the jacking end of the strand; the other components of the equation are factors reducing that force along the length of the strand. K is the wobble coefficient and is a result of unintended deviation in the strands expected to occur during installation, and ℓ_{px} is the distance from the jacking end to the point of interest. μ_p is the coefficient of friction between the strand and its sheathing, and α_{px} is the angle of curvature along the strand trajectory.

Table 2.1, from AASHTO LRFD Table 5.9.5.2.2b-1, lists recommended values for use in Eqn. 2-1. Wobble plays a small part compared with the frictional coefficient. Prestressing strand forces after initial stressing losses are discussed further in Chapter 3.

Table 2.1 Friction Coefficients for Post-Tensioned Tendons (For Use in Equation 2-1) (AASHTO LRFD Table 5.9.5.2.2b-1)

Type of Steel	Type of Duct	K	μ_p
Wire or strand	Rigid and semirigid galvanized metal sheathing	0.0002	0.15-0.25
	Polyethylene	0.0002	0.23
	Rigid steel pipe deviators for external tendons	0.0002	0.25
High-strength bars	Galvanized metal sheathing	0.0002	0.30

2.2 Greased and Sheathed Monostrand

Greased and sheathed monostrands are comprised of high-strength, low-relaxation steel strand encapsulated in a duct which is embedded in the concrete member. Each end of the strand is anchored to the concrete thereby transforming any tensile forces acting on the strand into compressive forces acting on the surrounding concrete. According to the Post-Tensioning Institute (PTI) (2006), some of the materials commonly used for the strand encapsulation include ferrous metals, HDPE or PP, all of which can be made into semi rigid or even flexible forms.

Greased and sheathed monostrands are used in the building industry, but are not commonly used in bridges.

For typical, current, post-tensioning projects flexibility is a desirable quality mainly for ease of construction. Most post-tensioned structures are designed with the post-tensioning installed in relatively straight lines, such as would be found in floor slabs, parking garages, or bridge decks. However, intentional deviations in the strand trajectory are quite common. By adding bends in a tensioned strand, the designer can customize the magnitude of the post-tensioning effect on member stresses.

Duct and strand flexibility is a very desirable quality with regard to this research. The average angle between the web and bottom slab of a typical box girder section is about 120 degrees, and the thickness of these components is less than 1 ft. These typical sections are made using preformed steel molds, making strand flexibility important for installation.

Several companies in the U.S. and abroad, including Dywidag-systems international (DSI), SWPC, and Suncoast, manufacture monostrands and their accompanying anchorage components. At each end of the monostrand is an anchor for transmitting the strand forces to the concrete member. Anchor design typically depends on the manufacturer or the conditions in which the anchor is expected to be utilized. Despite the multitude of possible shapes and sizes into which an anchor might be made, they all work by using a system of wedges that grip the strand as the strand attempts to relax after tensioning, similar in behavior to a Chinese finger trap. A brief description of how the monostrands are installed and what typical anchors may look like is in Appendix B.

For this project, the monostrand selected is manufactured in a greased and sheathed configuration, where the strands are coated with moisture resistant grease and are then inserted into a duct of slightly larger diameter. This type of monostrand is desirable because being coated with grease and then sheathed in production protects the strand from moisture before it leaves the facility and also facilitates the construction process. Because greased and sheathed monostrands are produced as a single unit with strand, duct, grease, and dead end anchor already in place, the crews preparing the concrete members for casting have fewer pieces to worry about, reducing the possibility for assembly errors to occur.

2.3 Typical Segmental Box Girder Bridges

One of the most efficient bridges in which to make use of monostrand technology is the segmental box girder bridge. As the name implies, the main characteristic of these bridges is a box-shaped girder running under the deck in the direction of traffic. It is the box or trapezoidal shape that provides much of the bridge's strength and efficiency. In addition, the top slab is cast as part of the box shape and provides the riding surface (roadway) for vehicles. Massive forms are created to cast the monolithic segment. Therefore, this bridge type is usually restricted to larger bridge projects because the cost of the form work can be distributed among all cast segments.

The Choctawhatchee (Mid-Bay) Bridge in Santa Rosa County, Florida exemplifies a typical segmental box girder bridge (Figure 2.2). The section contains two inclined webs, a top slab, and a bottom slab. Also shown in Figure 2.2 is the layout for the reinforcement steel. In addition, multi-strand tendons are used to post-tension the top slab transversely (perpendicular to traffic) and the cross-section longitudinally (in the direction of traffic). The longitudinal strands resist the self weight and traffic loads. The transverse strands are designed to resist transverse moments on either side of the webs.

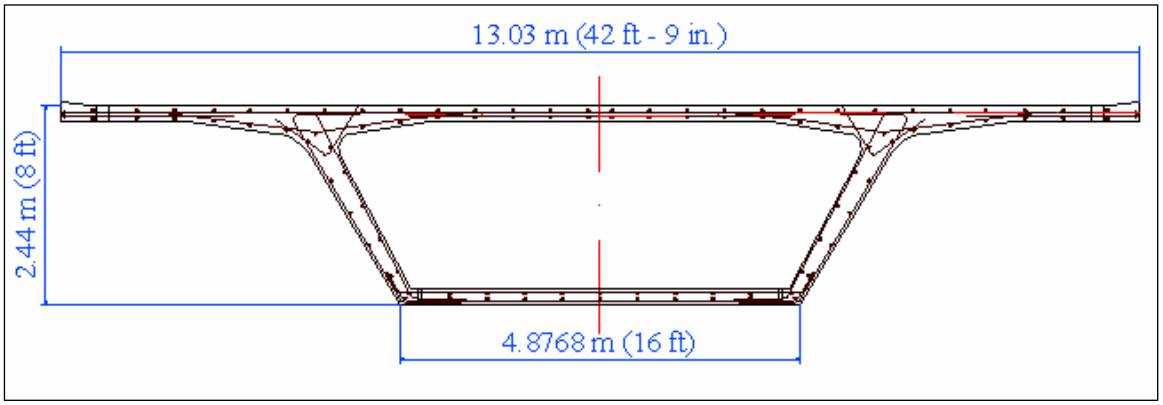

Figure 2.2 Typical Cross Section of Mid-Bay Bridge (Santa Rosa County, Fl.)

Figure 2.3 shows the deformations that would occur as a result of concentrated wheel loads being placed at the locations of the arrows: on the left are shown the deformations as a result of a large truck load placed in between the webs; on the right, the effect of a large truck load near the edge of the deck is shown.

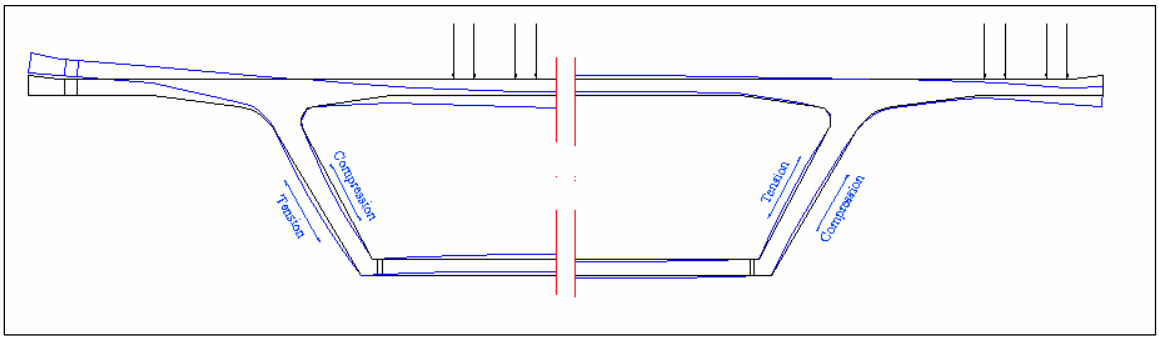

Figure 2.3 Effects of Transverse Bending
(Load Between Webs Shown on Left, Load on Cantilever Shown on Right)

The success of segmental box girder bridges is chiefly due to the use of post-tensioning to overcome tensile stresses in the concrete. Post-tensioning is provided in both the longitudinal and transverse directions, but typically not in the vertical direction (i.e., not in the webs). Most segmental box girder bridges rely on the use of standard deformed rebar to resist the shear forces in the webs. However, vertical post-tensioning (PT) bars are often used in the diaphragms, which are located over piers (columns), to help accommodate the multi-strand, longitudinal tendon anchorage forces.

PT bars can be used in the webs to resist shear forces. However, they are expensive to install. On the other hand, post-tensioned greased and sheathed monostrands could be used instead and would require only one strand, by anchoring the strand in the deck above one of the webs. The strand can then be directed down the first web, through the bottom flange and up the second web, back to the deck – in the shape of a "U". There are several benefits to using monostrands. Firstly, only one monostrand would be needed in the cross section, resulting in low material costs, low installation and jacking labor, and fast overall construction. The recently constructed

Metrorrey Viaduct in Monterrey, Mexico demonstrates the successful use of monostrands in a similar pattern.

2.4 The Metrorrey Viaduct

Figure 2.4 shows a U Cross Section segmental bridge. This bridge type takes advantage of the mandatory traffic barriers by placing the longitudinal post-tensioning in the traffic rails. This design reduces the overall depth of the structure but standard reinforcement would still be required in order to resist shear forces developed in the web sections of the bridge, now being played by the traffic rails. Another important setback to this technique can be summed up by the following quote, "Because the barriers have a crucial longitudinal function, they can no longer be replaced in service" (PTI 2006).

Figure 2.4 U Cross Sections for Segmental Bridge Construction (PTI 2006)

The Metrorrey Viaduct, completed in 2008, embraced the idea of the U-shaped cross section in a whole new way. Developed by Dr. Juan Jose Goni, P.E., Garcia Bridge Engineers, Inc., the Metrorrey Viaduct utilizes a U-shaped cross section to provide a low-impact travel way for light

rail cars. Goni stated, "Typical spans have a U-shaped cross section that allows the two rail tracks to be placed within the structure envelope, which reduces noise, danger of derailment, and visual impact" (Goni 2009). Goni's design depends on post-tensioned monostrands running transversely through the section instead of standard rebar. Figure 2.5 depicts the monostrand layout in one of the Metrorrey cross sections.

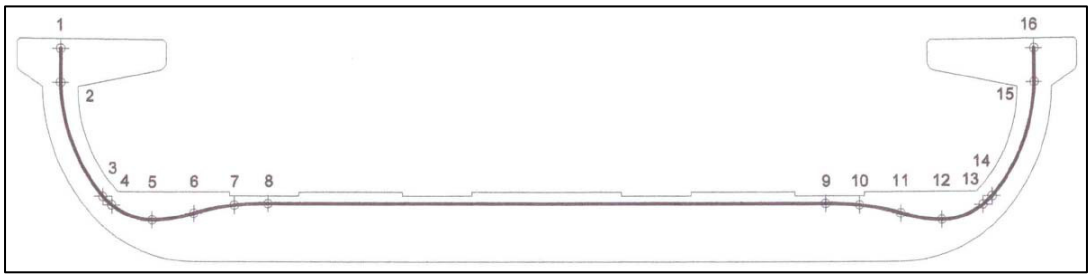

Figure 2.5 Cross-Section of Metrorrey Viaduct. Monterrey, Mexico

This layout provides the necessary compressive forces in the bottom slab and also resists shear forces in the webs. This cross section did not require excessive placement of standard rebar in the web sections, and a significant reduction in standard reinforcement resulted. "The typical segment contains only 45 kg of structural reinforcement per cubic meter of concrete (76 lb/yd^3) with # 3 bars, whereas most current light-rail segmental bridges typically contain concrete with a density of about 120 kg/m^3 (200 lb/yd^3)" (Goni 2009). As an added bonus, the placement of the anchor and jacking ends of the strands at the top of the webs allows for access for inspection, maintenance, or replacement of the strands. The Metrorrey Viaduct shows that using monostrands may be a viable alternative to standard rebar in the webs of segmental bridges.

2.5 Strength Loss from Bending

Most building materials, especially steel products, have been factory manipulated for best performance. For example, PTI (2006) explains that a process called *stabilizing* is used to increase the strength of steel wires in order to create Grade 270 strands. During this procedure,

the strand is strained to a pre-determined tension and then heated. As part of quality control for many projects, the ductility of strands might be tested according to PTI (2004) Specification 4130. This specification requires samples from a group of stay cables to be tested for ductility using the one-pin test (details of this test can be found in Appendix A). During this test, a length of strand is angled around a mandril and then placed under tension, to show that strands may be bent and still perform. The strand is bent to 160 degrees, which is much flatter than the 120 degrees that will be required for use in a segmental box girder.

Sumiden Wire Products Corporation (SWPC 2009) performed their own version of the one-pin test using different mandril sizes and different strand angles. Their testing concluded that as long as the diameter of the mandril, or in our case the bending diameter at the joint between web and bottom slab, was more than 25 times the diameter of the strand, then no appreciable loss of strength would be observed. Figure 2.6 illustrates the results of this research and the reason behind the 25-diameter rule.

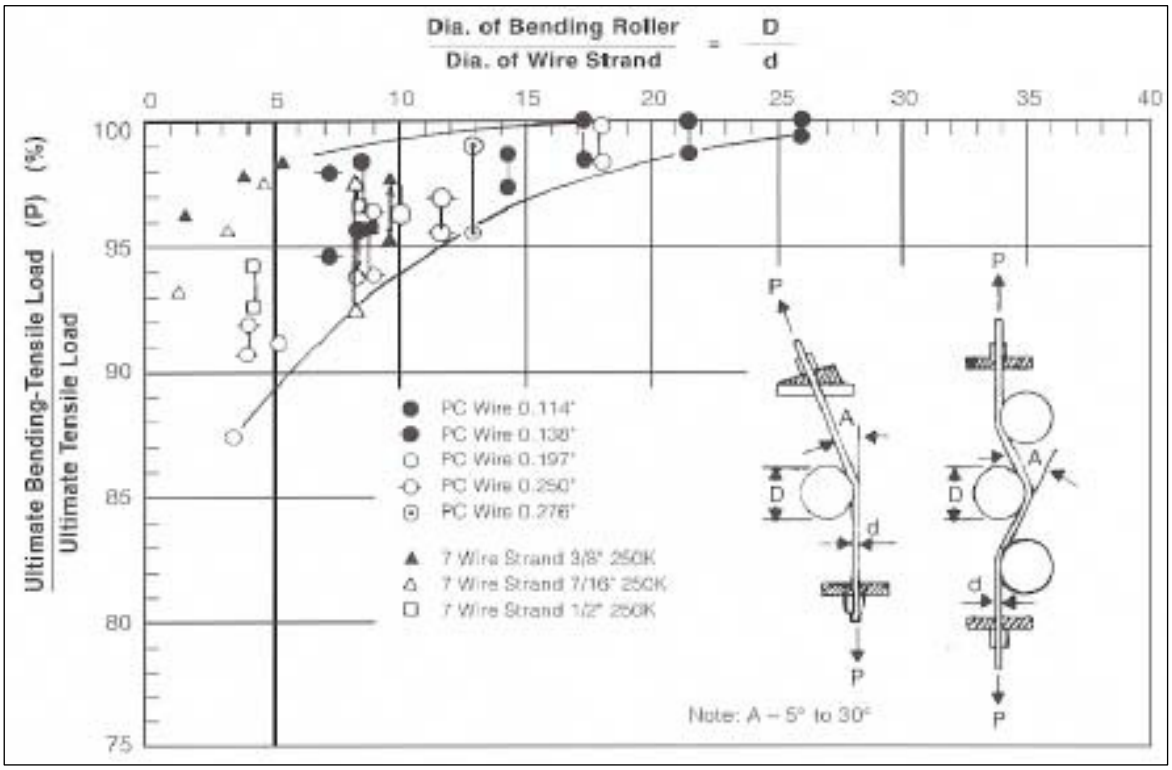

Figure 2.6 Sumiden Wire Products Corporation Results of Mandril Test (SWPC 2009)

In the Mid-Bay Bridge, there is ample room for the inclusion of a monostrand with a variety of angles and curve radii without any appreciable loss of strand performance. For simplification, the strand path shown in Figure 2.7 was selected. At a radius of 2 ft at the bottom slab-to-web intersection, the 0.6 in. diameter bent monostrand adheres to the 25-diameter rule.

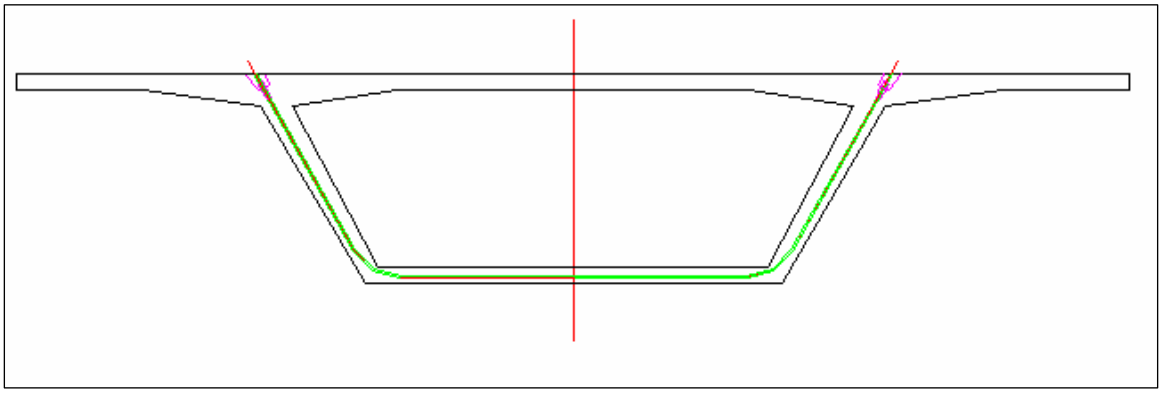

Figure 2.7 Proposed Monostrand Path in Typical Segmental Box Girder Bridge

2.6 Chapter Summary

This chapter discussed several different topics: post-tensioning systems, typical segmental box girder bridges, and a unique project completed in Mexico. Also, a reasonable monostrand path was selected for the example segmental box girder bridge. In Chapter 3, calculations to prove or disprove the viability of monostrand use is discussed, with regard to bent strand strength, prestressing losses, principal tension and compression stresses, and factored principal tension and compression stresses.

CHAPTER 3

ANALYSIS AND METHODOLOGY

3.1 Overview

This chapter quantifies stresses acting on a segmental box girder bridge in order to redesign a typical segment to rely on monostrands in the webs of the segment as opposed to large quantities of standard reinforcing steel. The analysis was based on uniting post-tensioned monostrand technology for web shear reinforcing, as used in the Metrorrey Viaduct, with the familiar technology of the segmental box girder bridge. For the analysis, the existing Mid-Bay Bridge cross section was used as the example bridge.

3.2 Analysis Description

To demonstrate the viability of replacing standard shear reinforcement with monostrands, a reasonable strand placement scheme was developed. Then, an analysis of stresses in the concrete member at the critical location in the web and along the span was performed. The unfactored, service stresses were compared to the allowable stress limits according to AASHTO LRFD Bridge Design Specifications (AASHTO 2007). Also, the factored stresses were compared to the modulus of rupture of the concrete to check for cracking.

3.3 Strand Placement

The monostrand was fit within the cross section of the example bridge. In Figure 2.7, a general representation of the strand layout and the closeness of fit are shown. Figure 3.1 shows that a 0.6 in. diameter greased and sheathed monostrand, bent at a 24 in. radius, can fit around the bottom slab-to-web corner, while maintaining a minimum 2 in. of concrete cover. The minimum radius required for a 0.6 in. diameter strand, per the 25-diameter rule, is 15 in.; a 0.7 in. diameter strand requires a minimum radius of 17.5 in. Therefore, providing a 48 in. bending diameter is adequate for either strand size.

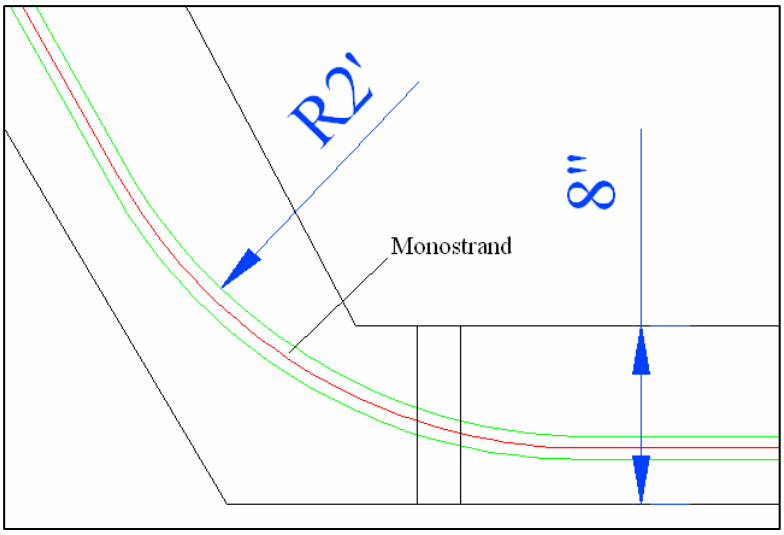

Figure 3.1 Mid-Bay Bridge Segmental Box Girder Corner Section with Monostrand

3.4 Mid-Bay Bridge Data

The Mid-Bay Bridge is a 19,265 ft long precast, post-tensioned, segmental concrete box girder bridge. It is located in Okaloosa County, Florida and serves as an over water route for motorists. The structure is composed of 138 approach spans each measuring 136 ft in length. Because this bridge was constructed using the span-by-span method, individual concrete segments were cast and then connected together to form a unit. Typical units are made up of four to six spans, with expansion joints located at each end of a unit. Individual precast segments are 42.75 ft wide, 17.75 ft long, and 8 ft deep. The webs are an average 1 ft thick and the entire segment was monolithically cast using 5500 psi concrete. The bridge was designed to support up to three lanes but is currently stripped for two twelve-foot lanes and two eight-foot shoulders. The majority of the bridge is at a relative height of 21 ft above mean sea level with a maximum elevation of 65 ft at the waterway channel.

This bridge was recently analyzed by Corven Engineering, Inc. to provide a load rating for the Florida Department of Transportation. For stress calculations in this research, their analysis was combined with new calculations. Details of these calculations are discussed in greater detail in following sections.

3.5 Calculating Strand Forces

Once the strand layout was selected, the forces along the monostrand's length were calculated in order to show that the tight radii at the bottom slab-to-web junction do not cause unacceptable prestressing losses. To solve for force along the length of a strand at certain points of interest, Equation 2-1 was used (see Section 2.1 for description of variables):

$$P_{Px} = P_{Pj} e^{-(K\ell_{Px} + \mu_P \alpha_{Px})} \tag{2-1}$$

Table 3.1 provides the values selected for use in this project. The values are the same as those assumed for the Metrorrey Viaduct project, which matched well with field measurements. The force in the strand, at various locations along its length, was calculated using an Excel spreadsheet.

Table 3.1 Strand Force Calculations Input Values (Goni 2009)

Wobble per m (K)	0.00035
Friction (μ_p)	0.042
Jack Stress (P_{Pj})	**82.00%**
Strand Diameter (in.)	0.6
Strand Area (in^2)	0.217
N Strands	1
f ult (ksi)	270
Tendon Modulus (ksi)	28300
Anchor Set (in.)	0.118

Because the majority of the monostrand's path follows a straight trajectory, it was not necessary to calculate the strand forces at minute increments along the entire strand length. Calculations of strand forces need to be performed mainly at locations where the angle of strand trajectory changes and at the strand ends. For example, the four strand segments shown in Figure 3.2 are Tendon Sections 3-6 in Table 3.2.

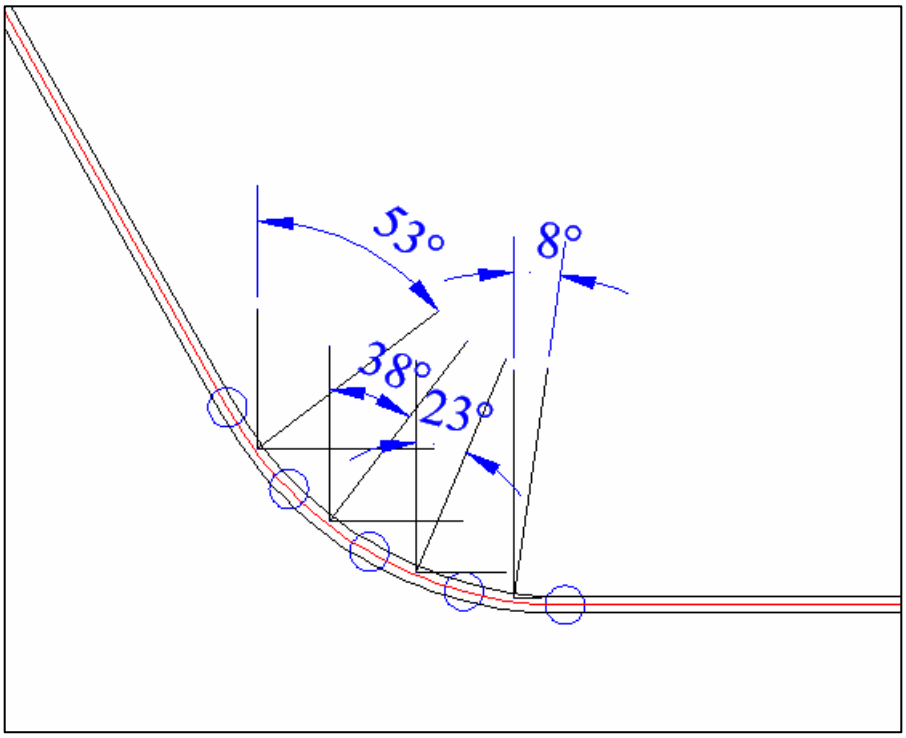

Figure 3.2 Mean Angles Between Points of Interest

Figure 3.2 shows the proposed strand path in the bottom corner of the typical segment. To the upper left, the monostrand follows the mean angle of the web and is straight. Once the strand reaches the topmost node, the strand trajectory slowly begins to change through the remaining nodes until becoming flat at the bottom slab of the segment. The mean angle of the monostrand between nodes was calculated (Figure 3.2). The calculations for force however, required the difference between the angles of the nodes; once converted to radians, these angles were then used to find the amount of force lost along the length of the monostrand (Table 3.2).

The values in the first four columns in Table 3.2 were obtained from Figure 3.2. The segment length column was found by measuring the length of monostrand between nodes. In the corner regions, the radius is 2 ft as decided upon before, and in straight regions the radius is zero. The resulting stresses at the jacking end (Tendon Section 1) were greater than the stresses at the dead end anchor (Tendon Section 16). To remedy this imbalance, it would be prudent to alternate the jacking side from monostrand to monostrand. For conservatism, the lower monostrand stresses were used when designing for principal web stresses, as discussed later.

Table 3.2 Monostrand Forces at Selected Points of Interest

				Before Anchor Set					
Tendon Section	L seg (in.)	Curve R (in.)	Defl. Angle (rad)	Tendon Stress (ksi)		Tendon Force (k)		Elongation (in.)	Lateral Force (k)
				start	end	start	end		
1	46.6	0.000	0.000	221.2	221.1	48.0	48.0	0.366	0
2	46.6	0.000	0.000	221.1	221.0	48.0	48.0	0.366	0
3	6.3	24	0.262	221.0	218.6	48.0	47.4	0.047	12.6
4	6.3	24	0.262	218.6	216.2	47.4	46.9	0.047	12.4
5	6.3	24	0.262	216.2	213.8	46.9	46.4	0.047	12.3
6	6.3	24	0.262	213.8	211.5	46.4	45.9	0.047	12.2
7	40.0	0.000	0.000	211.5	211.4	45.9	45.9	0.299	0
8	40.0	0.000	0.000	211.4	211.3	45.9	45.9	0.299	0
9	40.0	0.000	0.000	211.3	211.2	45.9	45.8	0.299	0
10	40.0	0.000	0.000	211.2	211.2	45.8	45.8	0.299	0
11	6.3	24	0.262	211.2	208.8	45.8	45.3	0.047	12.0
12	6.3	24	0.262	208.8	206.6	45.3	44.8	0.047	11.9
13	6.3	24	0.262	206.6	204.3	44.8	44.3	0.047	11.7
14	6.3	24	0.262	204.3	202.0	44.3	43.8	0.047	11.6
15	46.6	0.000	0.000	202.0	201.9	43.8	43.8	0.335	0
16	46.6	0.000	0.000	201.9	201.9	43.8	43.8	0.335	0
Total Strand Length (ft)		33.1			Total Elongation (in.)			2.97	

The second point of interest is that tensioning a strand around a bend induces radial (lateral) forces. In Table 3.2, the "Lateral Force" column shows the forces that this strand layout produces in the two bottom corner sections of the segmental box girder. These forces act on their corresponding nodes perpendicular to the strand at that node. Because these forces do not occur in the original box girder bridge design, a corner stress block was designed, as detailed later.

3.6 Section Properties and Stresses

Section properties -- cross-sectional area, neutral axis location, web width, first moment of area and moment of inertia -- were used to calculate axial, bending, and shear stresses in the webs. Axial stresses were calculated by dividing the axial force, P, by the cross-sectional area,

A. Bending stress at a point is equal to M*c/I, where M is the bending moment as a result of external loadings or self weight, I is the moment of inertia of the section, and c is the distance from the neutral axis of the beam to the point of interest. Shear stress was calculated from V*Q/(I*b), where V is the shear force, Q is the first moment of area, and b is the web width. These axial, bending, and shear stresses were then combined to calculate the principal web stresses, which were of interest in this study. Stresses were calculated at the top and bottom of the webs and at the neutral axis of the cross section; the top of the web was found to be the most critical section. Longitudinally, the critical location was at the first segment joint at the beginning of the first span in a unit.

The cross-sectional area, *A*, for the segment was determined to be 58.13 ft^2. The neutral axis is 2.48 ft from the top of the cross section. The web width, *b*, varied from top to bottom; at the critical location (top of web), it is 1.25 ft. The first moment of area, *Q*, at the neutral axis of the cross section is 73.34 ft^3 and is 71.58 ft^3 at the top of the web. The moment of inertia, I, was determined to be 487.1 ft^4.

3.7 Mid-Bay Bridge Live Loads

A crucial part of any bridge research and design is the determination of the live loads expected to act upon the structure. As opposed to dead loads, which are easily calculated using known values for the densities of concrete and steel, live load effects are calculated using AASHTO LRFD Bridge Design Specifications (AASHTO 2007). The live load effects were taken from the recent Mid-Bay Bridge load rating analysis that was performed for FDOT (Mid-Bay 2003); the computer program BDII was used for their analysis; and their results were verified in this study for accuracy or reasonableness. The loads were adjusted to conform to current bridge design specifications, by removing the 1.192 impact factor that was used in the load rating analysis for both truck and lane loads, and multiplying the truck load effects by the new impact factor 1.33. These live load effects are provided in Appendix C, and the live load results at the critical location are summarized in Table 3.3, along with the factoring required to use this data for further (stress) calculations.

Table 3.3 Live Load Forces

	HS20 Truck Load	HS20 Lane Load	HS20 Truck Load	HS20 Lane Load
Operation:	Shear	Shear	Moment	Moment
BDII Live Load Output (at critical location)	-184.96 k	-199.32 k	72.09 k	572.91 k
Remove Impact Load (1.192)	155.17 k	167.21 k	60.48 k	480.63 k
Live Load Factor (1.33)	206.38 k	167.21 k	80.44 k	480.63 k
Combined Live Loads	374 k		561 k	
Multiple Presence Factor (.85)	318 k		477 k	

3.8 Mid-Bay Bridge Dead Loads

The Mid-Bay Bridge dead loads include self weight, superimposed loads (barriers), initial post-tensioning, concrete shrinkage, creep, post-tensioning losses, and secondary post-tensioning effects. Post-tensioning losses are caused by the effects of concrete shrinkage and creep. The BDII analysis that was done for the load rating (Mid-Bay 2003) modeled the time-dependent effects due to creep and shrinkage.

From the BDII output, the dead loads from all of the sources aforementioned were summed together. Axial forces due to post-tensioning (PT) and PT losses were summed; likewise, dead load, live load, and post-tensioning shear forces were summed; and dead load, live load, and post-tensioning moments were summed. At the critical location (at the first segment joint near the first pier in the unit, at the top of the web), the dead load forces in Table 3.4 were obtained.

Table 3.4 All Applied Unfactored Dead Loads

Axial Forces	Shear Forces	Bending Moments
-4541.60 (k-ft)	-319.81 (k-ft)	-7222.39 (k-ft)

3.9 Stress Effects

Web stresses were the focus of this research. To be acceptable, these stresses must be lower than AASHTO LRFD Section 5.9.4.2 "allowable stresses", which are a function of the strength of the concrete. The Mid-Bay Bridge was constructed using concrete with $f'c$ = 5500 psi, resulting in AASHTO allowable stresses as summarized in Table 3.5.

Table 3.5 Allowable Stresses

Tension	$0.110\sqrt{f'c}$	37.1 ksf
Compression	$0.45f'c$	356 ksf

3.9.1 Shear Stress

The critical location for longitudinal shear was found to be at the first segment joint adjacent to the first pier in a typical unit. The shear forces obtained in Table 3.3 and Table 3.4 were converted to stress using the known relationship:

$$v = \frac{VQ}{Ib} \tag{3-1}$$

where v is the shear stress, V is the shear force, Q is the first moment of area, I is the moment of inertia, and b is the width of the section at the point of interest.

The shear stresses at the top of the web, neutral axis of the section, and bottom of the web are summarized in Table 3.6.

However, to calculate the principal stresses, the combination of both shear and normal stresses was considered.

Table 3.6 Possible Shear Stresses for Critical Location

	Location (ft) (relative to bottom of section)	***v* (ksf)**
$v = \frac{VQ}{Ib}$	6.750	37.504
	5.516	40.901
	0.583	36.68

3.9.2 Normal Stress

The normal stress at the critical location was determined as well by using the known relationship for normal stress, σ = -P/A +/- M*c/I, in which σ represents the normal stress, P is the tendon force on the cross section after all losses, A is the cross-sectional area, M denotes the bending moment, c is the distance from the neutral axis to the point in question, and I is the moment of inertia. The values for normal stress at the critical location are summarized in Table 3.7, where negative values denote compression.

The stresses in the first row of Tables 3.6 and 3.7 were used to determine the principal stresses, as discussed in Section 3.10; these stresses are at the critical location, i.e., at the top of the web at the first segment joint in the unit.

Table 3.7 Possible Normal Stresses for Critical Location

	Location (ft) (relative to bottom of section)	σ (ksf)
$\sigma = \frac{P}{A} - \frac{Mc}{I}$	6.750	-61.623
	5.516	-44.536
	0.583	-23.775

3.10 Principal Stresses

The term principal stress is used to describe a maximum state of axial stress, in which there is no shear stress. As stated in Chapter 2, concrete is much weaker in tension than it is in compression. In areas of high shear, a concrete member will crack most likely in the direction of the principal tension stress. The principal stresses were calculated using the shear and normal stresses, and then they were compared to the allowable stresses found in Table 3.5.

Shear and normal stresses were converted to principal stresses, σ_1 and σ_2, by using equations for transformation of stresses, or Mohr's Circle. Mohr's Circle is used to graphically describe the state of stress in an element in a member. The equation for the principal stresses is as follows:

$$\sigma_{1,2} = \frac{\sigma_x + \sigma_y}{2} \pm \sqrt{\left(\frac{\sigma_x - \sigma_y}{2}\right)^2 + \tau_{xy}^2} \qquad (3\text{-}2)$$

For the web stresses, σ_x denotes the longitudinal stress in Table 3.7; σ_y represents stress as a result of vertical loading (this will be explained later and is due to transverse bending and also the vertical web force caused by the monostrands); and τ_{xy} represents the shear stress acting on the element from Table 3.6.

3.10.1 Longitudinal Shear and Bending

Without transverse bending effects and monostrands, σ_y is equal to zero. The resulting principal stresses were 79.3 ksf compression and 17.7 ksf tension.

3.10.2 Effects of Transverse Bending

The effects of transverse bending are illustrated in Figure 2.3. Transverse post-tensioning resists bending in the top slab. However, in a typical segmental bridge, web reinforcing steel resists bending at the web-top slab intersection. The two modes for obtaining the greatest tension on the web faces being questioned is to place a military vehicle on the cantilever, or two HL93 lanes in between the webs.

3.10.3 Transverse Bending and Longitudinal Stresses On Inner Web Face

On the right hand side of Figure 2.3, the load effects on the web as a result of a load being placed on the cantilever are shown. This configuration will cause tensile forces to form on the inner face of the webs. Loads affecting the magnitude of the moment at the top of the webs include dead loads, concrete barriers, live loads, and transverse post-tensioning forces. The moments at the top of the web due to dead load, barriers, military vehicle live load, and transverse post-tensioning -- per linear foot of segment -- are -1.27 k-ft, 5.77 k-ft, 6.83 k-ft, and -0.44 k-ft respectively. By summing all of these moments, the moment acting at the top of the web was obtained.

The moments at the top of the webs cause stresses on the web faces. The normal stress was calculated on each web face, using section properties of the web, which is 1.083 ft thick (Figure 3.3 shows the top of the web at the top slab-web junction).

The normal stress, σ_y, was calculated to be 55.7 ksf tension on the inside face of the webs. This tensile stress was combined with the longitudinal shear and bending stresses calculated previously. The new principal stresses were 66.7 ksf tension and 72.6 ksf compression.

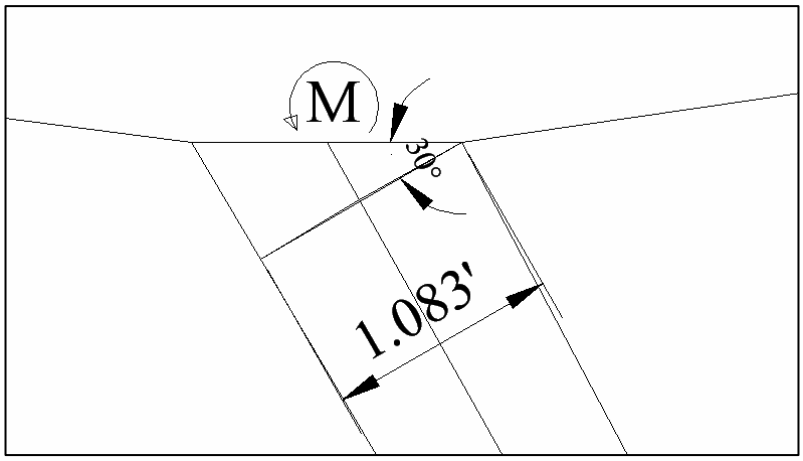

Figure 3.3 New Web Stress Plane

3.10.4 Transverse Bending and Longitudinal Stresses On Outer Web Face

The process for determining the stresses acting on the outer web face was the same as that used to determine the inner web face stresses. The same moments due to dead load, barriers, and the transverse post-tensioning were used. However, for the live load, two HL93 trucks were placed between the webs at the point in which they cause the maximum moments at the top of the webs (-10.79 k-ft/ft). This moment was combined with the moments from the other transverse loadings, resulting in a total moment of -6.73 k-ft/ft. The normal stress, σ_y, was calculated to be 34.4 ksf tension on the outside face of the webs. This stress effect was combined with the previously calculated shear and normal stresses due to longitudinal forces, and new principal stresses on the outside web faces of the segment were calculated to be 47.3 ksf tension and 74.5 ksf compression.

3.11 Factored Principal Stress vs. Modulus of Rupture

If Strength I limit states are applied, all dead loads (self weight, superimposed dead loads, creep, and shrinkage) are multiplied by a factor of 1.25, post-tensioning effects remain

unchanged (or factored by 1.0), and live loads are magnified by a factor of 1.75. The factored load effects acting on the critical section are given in Table 3.8.

Table 3.8 Unfactored vs. Factored Loading

	Original Loads		Factored Loads	
	Shear	Moment	Shear	Moment
Dead Load	320 k	-7222 k-ft	453.7 k	-6834.4 k-ft
Live Load	318 k	477 k-ft	555.8 k	3851.2 k-ft

The above factored force effects were used to determine the "factored" principal stresses. The tensile principal stress were compared to the concrete modulus of rupture to check if the concrete will crack under factored load conditions; and the compressive principal stress was compared to the allowable compressive stress for concrete. The concrete modulus of rupture and allowable compressive stress are provided in Table 3.9.

Table 3.9 Modulus of Rupture

Tension	$0.24\sqrt{f'c}$	81.1 ksf
Compression	$0.45f'c$	356 ksf

3.11.1 Transverse Bending and Longitudinal Stresses On Inner Web Face

Principal stresses that include the influence of transverse bending were calculated. The transverse bending moments and, subsequently stresses, on both the inner and outer web faces were factored using the Strength I limit state load factors. Table 3.10 serves as a summary of these moments and the factors that were applied to each load effect.

Table 3.10 Factored Transverse Moments (Inner Face)

	Unfactored Value	Factor	Type	Strength I Limit Value
Dead Load	-1.27 k-ft	1.25	Dead Load	-1.59 k-ft
Barriers	5.77 k-ft	1.25	Dead Load	7.21 k-ft
Military Truck	6.83 k-ft	1.75 1.2	Live Load Multiple Presence	14.34 k-ft
Post-Tensioning	-0.44 k-ft	1.0	Post-Tensioning	-0.44 k-ft

From the sum of the forces in the Strength I Limit Value column of Table 3.10, the normal stress along the web axis, on the inner web face, was obtained. The principal stresses as a result of this load combination were found to be 118.7 ksf tension, and 82.7 ksf compression.

3.11.2 Transverse Bending and Longitudinal Stresses On Outer Web Face

In order to find the stresses acting on the outer web face, the steps from Section 3.11.1 were repeated. The resulting transverse bending moments using the Strength I limit state load factors are summarized in Table 3.11.

Table 3.11 Factored Transverse Moments (Outer Face)

	Unfactored Value	Factor	Type	Strength I Limit Value
Dead Load	-1.27 k-ft	1.25	Dead Load	-1.59 k-ft
Barriers	5.77 k-ft	1.25	Dead Load	7.21 k-ft
Military Truck	-10.79 k-ft	1.75	Live Load	-18.88 k-ft
Post-Tensioning	-0.44 k-ft	1.0	Post-Tensioning	-0.44 k-ft

From the sum of the forces in the Strength I Limit Value column of Table 3.11, the normal stress along the web axis, on the outer web face, was obtained. The principal stresses as a result of this load combination ware found to be 92.2 ksf tension and 85.9 ksf compression.

3.12 Chapter Summary

The purpose of this chapter was to provide an analysis of an existing segmental box girder bridge, to which modifications can be made to the segment's web reinforcing steel. To meet this objective, the maximum principal stresses acting at critical locations within the segment webs were calculated, using service level stresses with all load factors equal to 1.0. The principal stresses were recalculated using factored loads from the Strength I limit state, where all load factors were greater than or equal to 1.0. These stresses were of greater magnitude and were included specifically to insure that any design efforts regarding this structure did not result in cracking of the concrete. At this point, the stresses acting on the segment in the longitudinal, transverse, and vertical directions were all quantified for the segment without the inclusion of the proposed monostrand.

CHAPTER 4

RESULTS AND MODIFICATIONS

In the previous chapter, stresses in an example bridge were quantified. The purpose of this chapter is to compare the quantified stresses with the allowable values, then to design the segment for the inclusion of monostrands within the webs of the structure. These principal stress results are summarized in Table 4.1 and are discussed in the following sections.

Table 4.1 Principal Stresses without Web Monostrands (+ indicates tension; - indicates compression)

		Principal Stresses vs. Allowable Stresses		**Factored Principal Stresses vs. Modulus of Rupture**	
		Load Factors: Dead load = 1.0 Post-Tensioning = 1.0 HL93 Live Load = 1.0	Allowable Stresses: 1.77 Mpa (37.1 ksf) -17.1 Mpa (-356 ksf)	Load Factors: Dead Load = 1.25 Post-Tensioning = 1.0 HL93 Live Load = 1.75	Modulus of Rupture: 3.88 Mpa (81.1 ksf) -17.1 Mpa (-356 ksf)
		Principal Stresses	OK or Not Good (NG)	Principal Stresses	OK or Not Good (NG)
Longitudinal Shear and Bending	(either web face)	σ_{max} = 17.7 ksf	OK	σ_{max} = 35.1 ksf	OK
		σ_{min} = -79.3 ksf	OK	σ_{min} = -98.8 ksf	OK
Transverse Bending + Longitudinal Shear and Bending	(on inner web face)	σ_{max} = 66.7 ksf	NG	σ_{max} = 118.7 ksf	NG
		σ_{min} = -72.6 ksf	OK	σ_{min} = -82.7 ksf	OK
Transverse Bending + Longitudinal Shear and Bending	(on outer web face)	σ_{max} = 47.3 ksf	NG	σ_{max} = 92.2 ksf	NG
		σ_{min} = -74.5 ksf	OK	σ_{min} = -85.9 ksf	NG

4.1 Principal Stress Summary

The principal stresses obtained throughout the previous chapter are summarized in Table 4.1. For the Longitudinal Shear and Bending case, both service level principal tension stresses and factored principal tension stresses were acceptable because they were less than the allowable stress and modulus of rupture, respectively. However, when transverse bending was included, both the inner and outer web face principal tension stresses (service level and factored) exceeded the allowable stress and modulus of rupture, as designated in the table by shading. For all load cases, the principal compression stresses were acceptable. The existing segment includes standard steel reinforcing; however a new design based on web monostrands was explored, to reduce the principal tension stresses for both service level and factored conditions.

4.2 Monostrand Web Effects

The stress transformation equations were used to determine the new stresses after the effects of the monostrands were considered. The compressive stress that the web monostrand is expected to impart along the web's axis is found as follows:

$$\sigma_{y(\text{strand})} = \frac{P_{\text{strand}}}{s * t_{\text{web}}} \tag{4-1}$$

where σ_y represents the vertical stress imparted to the web as a result of the monostrand forces within the web denoted by P_{strand}. Because the stress within the member is found by dividing the applied forces by the area resisting the forces, the variables s and t_{web} are the spacing between strands and the web thickness at the point of analysis, respectively.

The monostrand is a 0.6 in diameter, low-relaxation, 270 ksi 7-wire strand that is greased and sheathed. These monostrands typically are stressed at approximately 65% of their ultimate strength in service after all losses have been considered. The strands do exhibit a reduced force at the anchored dead (non-jacking) end, which means that in order to be conservative, this lowest

force was used as a starting point to modify the stresses that were already calculated. A layout of strands at one foot spacing was used. The strands were staggered within the web as shown in Figure 4.1. By using this configuration, the one foot spacing can be maintained without crowding the strands; alternating the strands cancels effects caused by strand eccentricity.

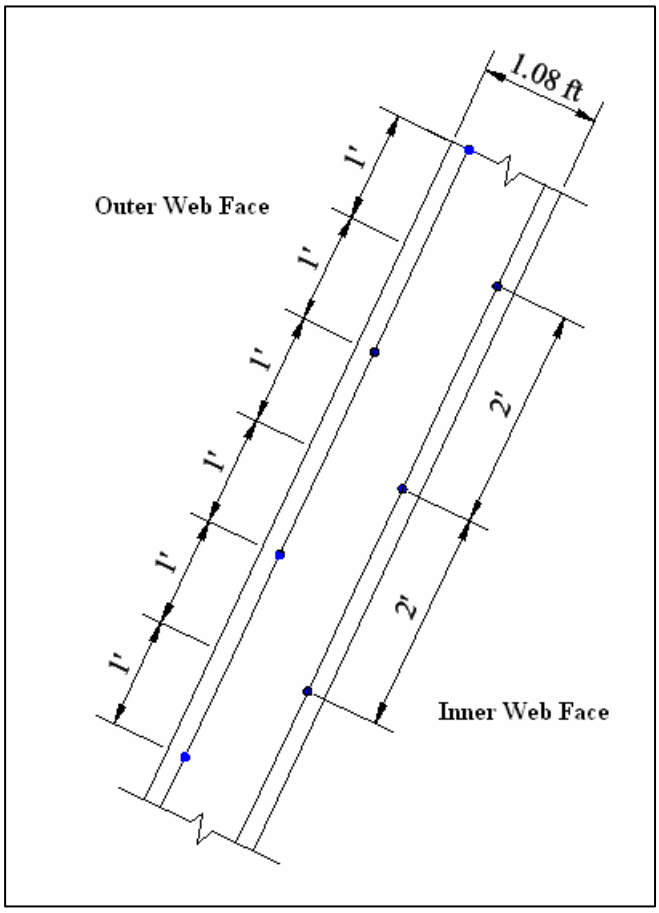

Figure 4.1 Web Monostrand Layout

4.2.1 Unfactored Load Effects

This section follows the same procedure for calculating principal stresses on the web faces as found in Section 3.10.3. The axial stress caused by the web monostrand and transverse bending was calculated from:

$$\sigma_y = \frac{P}{A} + \frac{Mc}{I} \tag{4-2}$$

In previous sections, before the inclusion of monostrands, the normal stress along the axis web, σ_y, contained only the influence of transverse bending on the web and no axial force. For this portion of the research, this term also contained the new post-tensioning force of the web monostrands over the tributary area over which the force takes effect.

Taking 65% of f_{ult} to be 175.5 ksi, the force per strand was determined using the strand area. Application of Equation (4-1) then revealed the compressive stress applied to the web by the monostrand. This resulted in a reduced principal tensile stress of 34.9 ksi.

The same steps were followed for the outer web face stresses resulting in a new principal tensile stress of 16.8 ksf in the outer web face.

4.2.2 Factored Load Effects

The procedure for including the monostrand forces into the equations for principal stresses was the same as that followed for the unfactored forces, except that the dead and live loads were factored; a load factor of 1.0 was used for the monostrand forces. The new principal tensile stress on the outer web face was determined to be 62.3 ksf and on the inner face, 87.2 ksf.

For this monostrand design, the addition of the web monostrands resulted in acceptable values of stress for all situations except for Strength I limit state inner web face tension. The magnitude of the tensile stress was so close to the limit however, that further exploration proved necessary. Using a concrete strength of 6500 psi results in a modulus of rupture of 87.1 ksf, which is about equal to the principal tensile stress. In addition to these measures, alternative monostrand spacing could be explored.

4.3 Shear Strength

The last section showed that adding web monostrands resulted in large reductions in web tensile stresses. Strength I limit state factors were used to ensure that the segment that would not

crack under factored load conditions. In case cracking did occur, it is only prudent to verify the ability of the web monostrands to withstand the effects of longitudinal shear. Because the shear strengths provided by reinforcing steel and by monostrands are both proportional to $A_s f_s/s$, Equation (4-3) was used to evaluate the feasibility of replacing reinforcing steel with monostrands. In Eqn. (4-3), A_s is the cross-sectional area of the steel, f_y denotes the yield strength of the steel, and s is the spacing between steel reinforcing or monostrands.

$$\left(\frac{A_s f_y}{s}\right)_{\text{reinforceing steel}} = \left(\frac{A_s f_s}{s}\right)_{\text{monostrands}} \tag{4-3}$$

The current Mid-Bay shear reinforcement consists of #5 bars spaced at 12 in. along both the outer and inner web faces. Using Equation 4-3, the existing bars and the proposed monostrands were compared. The Grade 60 bars currently being used provide a ratio of 37.2 k/ft whereas the monostrands, assumed to have act at the lowest value of 176 ksi, provide a ratio of 38.3 k/ft. This comparison showed that in terms of shear the proposed monostrands can meet the shear demands of this bridge.

Some web reinforcing would still be needed to control cracking and to act as skin reinforcing. Welded wire reinforcement could be explored to satisfy this purpose.

4.4 Monostrand Corner Restraints

Thus far monostrands placed in the webs were proven to improve the resistance of the structure to detrimental tensile effects. However, force effects that were touched upon earlier in Chapter 2 describing the lateral effects of a tensioned cable around a bend have not yet been analyzed. In the monostrand's current layout, there is only a small amount of concrete cover on the monostrand on the inside corner. It is assumed that this layout within the existing segment cross section will result in rupture of the concrete in the inside bottom corners of the cross section. To resist these forces, a concrete corner fillet was designed to restrain the monostrand.

For a corner fillet (block) to satisfactorily meet the requirements of this project, the block

must have sufficient anchorage into the corner of the girder to resist the tear-out forces from the monostrand.

4.4.1 Fillet Dimensions

Figure 4.2 shows an example corner fillet designed to resist the tear-out forces that the monostrand is expected to impose on the inside bottom corner of the segment due to radial forces.

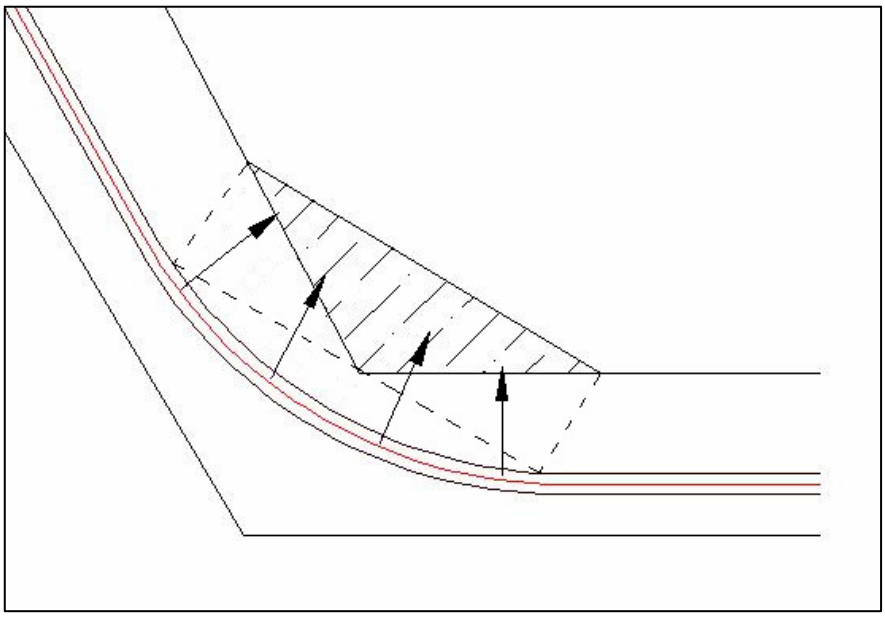

Figure 4.2 Corner Block with Force Vectors

The hatched area in Figure 4.2 is the additional concrete to support the lateral forces from the monostrand. The total area of concrete acting to resist the lateral strand forces is contained within the dashed lines forming a rectangle below the corner fillet and a circular segment between the rectangle and curved monostrand. The rectangle and segment together provide 1.38 ft^2 of concrete, per face, in the plane of the monostrand. As seen in Figure 4.3, this value is conservative as concrete would likely fail along a larger area, denoted by the dashed lines.

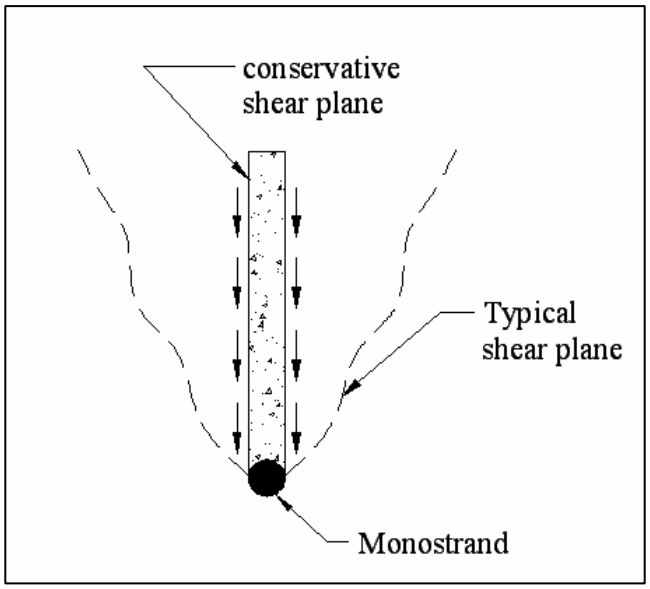

Figure 4.3 Shear Planes within Corner Fillets

4.4.2 Fillet Shear

From Table 3.2 the lateral forces developed as a result of curving the monostrands is quantified between each node selected for analysis. The largest corner forces before anchor set were summed. A force of 49.5 kips was obtained from the summation and was then used in conjunction with ACI equation 11-3, represented here as Equation 4-4, to back substitute for the necessary concrete area required to resist the monostrand pull-out.

$$V_c = 2\sqrt{f'_c} * A \tag{4-4}$$

Equation 4-4 is usually used to determine the nominal strength provided by concrete where V_c represents the nominal strength, f'_c denotes the concrete strength, and A is the cross-sectional area of the concrete failure plane that resists the applied forces. In accordance with ACI Section 9.3.2.3, Eqn. 4-4 is multiplied by a resistance factor of 0.75. From this operation it was determined that a minimum area of 1.545 ft^2 per face is required. The two-foot long fillet

recommended can resist up to 44.2 kips. Additional shear reinforcement in the form of standard reinforcement is required to withstand the remaining 5.3 kips.

In order to use standard reinforcement to resist shear perpendicular to the reinforcement ACI equation 11-25 (Eqn 4-5) was used, where V_n is the nominal shear strength provided by the reinforcement, A_{vf} is the cross-sectional area of the reinforcing bars, f_y is the yield strength of steel, and μ is the frictional coefficient. The corner fillets could be cast monolithically with the rest of the segment and not added later. Therefore, in accordance with ACI 11.7.4.3, μ is taken to be 1.4λ, where $\lambda = 1.0$ for normal weight concrete.

$$V_s = A_{vf} * f_y * \mu \tag{4-5}$$

The resulting demand for steel reinforcement can be satisfied by the inclusion of one #3 reinforcing bar per corner fillet, laid longitudinally within the box, however, two #3 or #4 bars are recommended.

4.5 Chapter Summary

The goal of this chapter was to show how modifying a segmental box girder bridge cross section with web monostrands could yield reduced principal tension stresses in the webs. The new design shows that replacing web reinforcing steel with web monostrands is feasible in terms of both principal tension stresses being less than maximum allowable stresses and shear strength.

CHAPTER 5

CONCLUSIONS AND RECOMMENDATIONS

Chapters 3 and 4 covered the initial analysis and subsequent modifications that were made to the example bridge in an attempt to improve the design. In this chapter, conclusions will be made, followed by additional topics such as other concerns and cost comparisons. Finally, possible future works and a summary will be provided.

5.1 Initial Conclusions

Table 5.1 recounts all of the principal stresses that were found in the webs of the cross section. In this rendering however, the principal stresses that had violated the respective limits were reduced by the compressive forces imposed on the webs by the monostrands. The two principal stresses that exceeded the allowable stress limits were both reduced to acceptable levels. Only the Case II value from the Factored Principal Stresses column was reduced to an acceptable level by monostrand inclusion alone. However, for the remaining Case I value from the Factored Principal Stresses column to be acceptable, additional modification was needed to strengthen the structure to resist the tensile principal stresses within the webs. Case I tensile stress may be deemed acceptable by also using a 6500 psi concrete design mix as opposed to 5500 psi.

Figures 5.1 and 5.2 illustrate the differences between the old and the new web reinforcement. In Figure 5.1 the standard #5 bars are shown on both the inner and outer web faces for the two webs. Figure 5.2 shows how the monostrand is fit into the section and includes two thin layers of welded wire to provide the necessary skin reinforcement.

5.2 Cost Comparison

The current reinforcing steel installed in the Mid-Bay Bridge weighs roughly 2.1 lbs per square foot of web surface area. Estimated at $0.71 per pound, including installation costs, the resulting cost for standard web reinforcement is about $1.50/sf of web area. Accurate data

concerning cost of monostrands for bridge use is not readily available, so for this comparison the cost of multiple-strand tendons will be used: $2.75 per pound. This would result in a cost of $2.00/sf of web surface area for the monostrand that was analyzed for use in the example bridge. This is a rough estimate, in that the unit cost used was not for monostrands, but rather for multiple-strand tendons, which require different hardware, larger jacking equipment, and specialized grouting operations.

Table 5.1 Principal Stresses Including Web Monostrand Benefits

		Principal Stresses vs. Allowable Stresses		**Factored Principal Stresses vs. Modulus of Rupture**	
		Load Factors: Dead load = 1.0 Post-Tensioning = 1.0 HL93 Live Load = 1.0	Allowable Stresses: 1.77 Mpa (37.1 ksf) -17.1 Mpa (-356 ksf)	Load Factors: Dead Load = 1.25 Post-Tensioning = 1.0 HL93 Live Load = 1.75	Modulus of Rupture: 3.88 Mpa (81.1 ksf) -17.1 Mpa (-356 ksf)
		Principal Stresses	OK or Not Good (NG)	Principal Stresses	OK or Not Good (NG)
Longitudinal Shear and Bending	(either web face)	σ_{max} = 17.7 ksf	OK	σ_{max} = 35.1 ksf	OK
		σ_{min} = -79.3 ksf	OK	σ_{min} = -98.8 ksf	OK
Transverse Bending + Longitudinal Shear and Bending	(on inner web face)	σ_{max} = 34.9 ksf	OK	σ_{max} = 87.2 ksf	NG
		σ_{min} = -72.6 ksf	OK	σ_{min} = -82.7 ksf	OK
Transverse Bending + Longitudinal Shear and Bending	(on outer web face)	σ_{max} = 16.8 ksf	OK	σ_{max} = 62.3 ksf	OK
		σ_{min} = -74.5 ksf	OK	σ_{min} = -85.9 ksf	NG

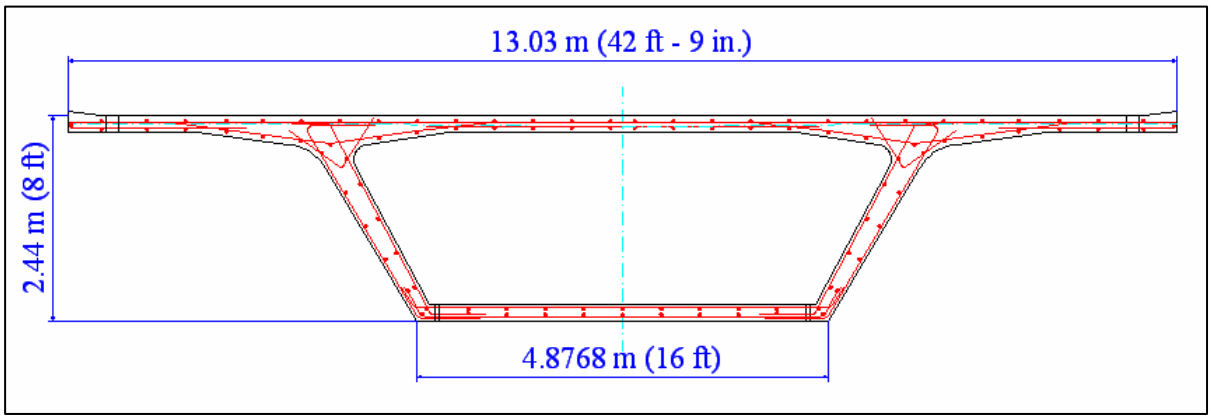

Figure 5.1 Original Reinforcement Layout

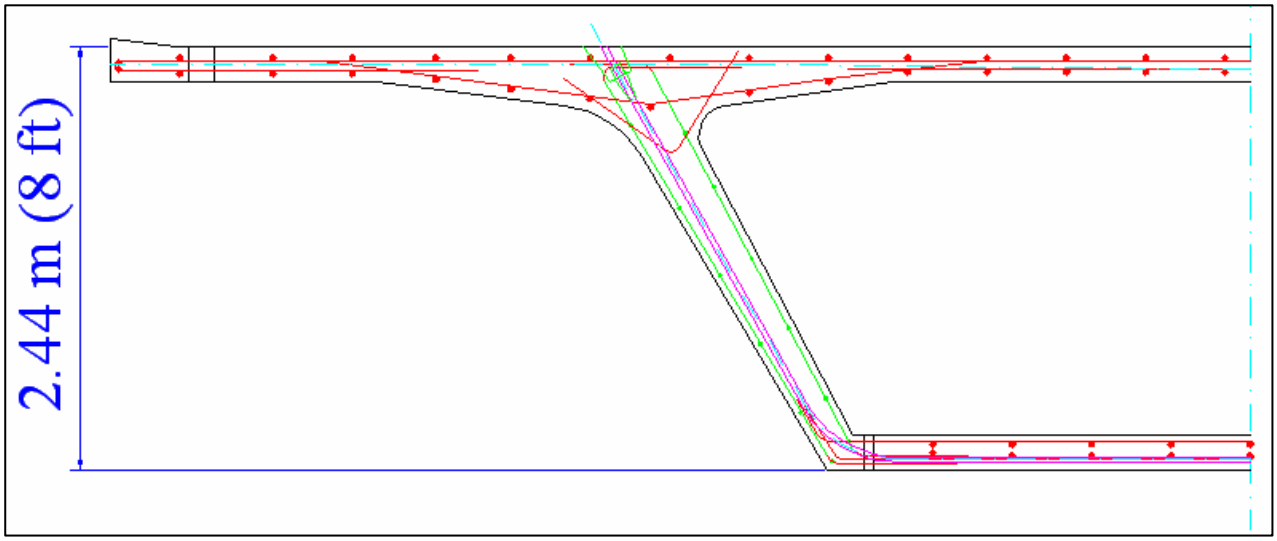

Figure 5.2 New Web Monostrand and Reinforcement

At face value it would seem that the standard reinforcing would be the more lucrative alternative, however, the benefits of using monostrand range from fewer number of monostrands being used than rebar, i.e. one monostrand per foot compared with four #5 bars per foot, to reduced labor in terms of tying segments prior to casting. Benefits would continue to be realized as a greater number of bar bends is specified. Multiple bar bend details and variable segment cross sections may sway the cost alternative more in favor of the monostrands.

5.3 Other Concerns

Resistance to corrosion is naturally a vital quality for the post-tensioning system to possess. All post-tensioning systems exhibit some form of moisture ingress defense mechanism, the two most popular are grouting and, as discussed, grease and sheathing. A review of the structure shows no reason why one system should be used over the other. However, installation of post-tensioning in the webs of the segmental box girder will do something to the strand that is almost never done in current practice.

In typical building applications where the strand lays flat, the jacking end is tucked into a hollowed out section of concrete created by a plastic pocket former. This pocket is shaped like a cup facing sideways, even if moisture were to penetrate the grout plug the 'cup walls' and gravity would influence the moisture to drain out along the bottom wall of the cup. For the installation suggested by this research the cup shaped pocket would be facing in an upward direction catching water, making moisture protection a much greater concern (see Figure 5.3).

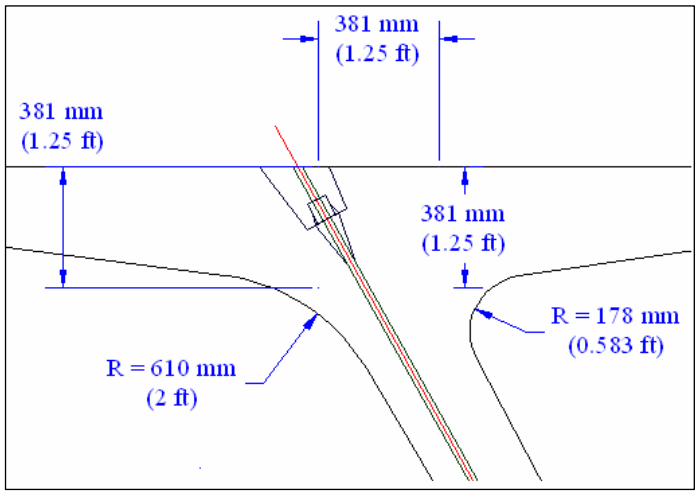

Figure 5.3 Monostrand Anchorage in Top Slab

The obvious solution is to fill the strand with a moisture blocking material such as grease or grout. Grease and sheathing is recommended for this application because this method requires a much smaller diameter sheathing that a grouting system; it also coats the strand and chemically

blocks the corrosive action of moisture while reducing the effect of friction on the strand especially in the bottom corners of the box. Even with these protective measures in place, there could be potential for moisture ingress at the anchor. In the Metrorrey Viaduct, where monostrands were used, the ends of the strands are not subjected to any large repetitive impacts such as train or vehicle loads. This is not to say that this technology should not be used, but that prudent use of this technology would require additional research into the realm of anchorage integrity under repeated impact and possible increased exposure to moisture.

5.4 Alternative Design

This research was intended to determine the benefits of using monostrands in a segmental box girder bridge using the strand layout in Figure 2.7. However, given the possible concerns that arise regarding anchorages exposed to new loads and moisture, an alternative design is proposed for additional research (Figure 5.4).

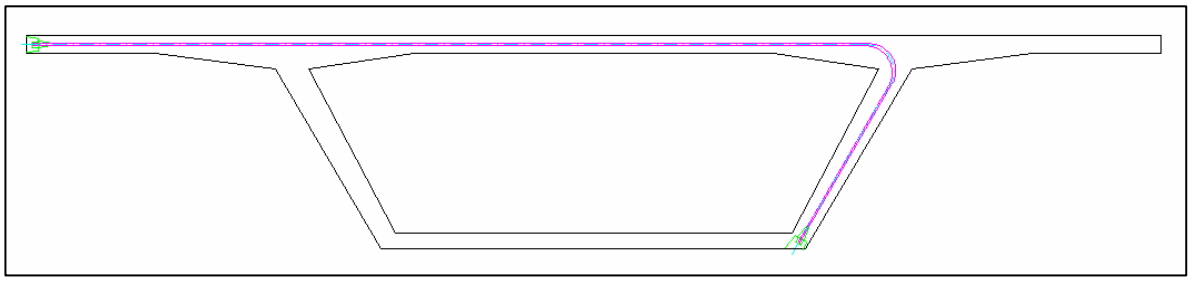

Figure 5.4 Alternative Monostrand Layout

In this design the monostrand provides compressive forces to both the deck and the webs. The anchors are also installed in a way as to prevent any traffic loads or excessive exposure to moisture. However, this design was not primarily considered because of the excessive bend in the monostrand which would cause more losses in strand axial force and development of lateral forces in the top corner of the segment.

5.5 Future Work

Practicality of the new design will ultimately depend on the strength, labor, and cost. In terms of strength, this research showed that the new design is feasible. This is no surprise because the research proposed to place every portion of the segment under a compressive stress including the webs. In comparison with standard deformed bars, the post-tensioned monostrands impose a beneficial load to the webs whereas the standard rebar only contribute once the concrete has begun to crack.

In terms of cost savings much can still be learned. During the course of the research several estimators were contacted in order to determine accurate price estimates for using monostrands. All of the estimators were unable to help, citing cost information as private and proprietary. Therefore the costs that were used in this research are rough estimates and should warrant further research.

This proposed monostrand layout would also require further research in terms of ease of constructability or labor. It is true that in standard monostrand applications labor is usually minimal, because strands are normally laid out in straight lines. However, it might prove to be more labor intensive to bend a monostrand around a tight radius that to bend and tie standard rebar. This is a topic that should be further investigated.

5.6 Chapter Summary

This chapter began with covering the conclusions that could be made by a review of the data. From that review it was revealed that the proposed monostrand layout is a viable alternative to using standard deformed rebar within the webs of segmental box girder bridges. This chapter also touched upon a few topics that could pose new difficulties for the utilization of this technology in our current segments; however, these new difficulties may be easily improved upon.

If these possible difficulties are examined under the view point of future work, then these considerations might just be another small step towards utilizing post-tensioning technology within the webs -- resulting in a more efficient, and possibly less expensive segmental box girder bridge.

APPENDIX A

DETAILS OF "ONE PIN TEST"

This test provides a measure of the ductility of 12.7 mm and 15 mm diameter 7-wire strands.

Section 4.2 of the recommendations requires that the fatigue strength of the stay cable system be demonstrated by tests of at least three stay cable specimens. Passage of these tests does not insure similar properties for all of the strand produced for the project.

Application of the "One-Pin Test" to each manufactured length of strand gives much better assurance as the ductility of that length of strand. In this instance, the term ductile strand means a strand with minimum notch sensitivity. Low notch sensitivity is essential for strands or wires held in wedge type grips and subjected to repeated loads.

Section 3.2.2.1 requires tests on "each manufactured length, or every 10 Mg (whichever is less)." Two apparently identical wires from the same heat of steel can have very different properties in their final condition. If, for instance, one or more of the cooling blocks in the wire drawing machine get too hot, the resulting wire will have very poor ductility, but this will not be visible to the eye. Strand with wire of this type would fail the "One-Pin Test."

Several procedures for checking notch sensitivity were investigated during preparation of the 1986 Edition of these Recommendations. It was concluded that the "One-Pin Test" is the only one that adequately measures notch sensitivity. FIP* had established the details of the "One-Pin Test" as a standard and they leave it to each specification to establish the degree of pin test efficiency required for the application in question.

Test Procedure:

Cut a strand sample long enough for two ultimate strength tests and three pin tests.
Load one piece to failure and record actual ultimate strength = f'_{sa}.
If first test fails at the grip, load a second sample to failure.
Use the highest value as f'_{sa}. This value is not acceptable if the elongation in 610mm does not exceed 3.5%.
Load a sample to failure in the pin test device and record the load at failure as F_R. Loading speed shall be uniform and not greater than 30 MPa per second.
Pin Test Efficiency (PTE) = F_R/f'_{sa}
The PTE for strand used in stay cables shall not be less than 80 percent (See Section 3.2.2.1).
Details of the one-pin device are shown in Figures A.1 and A.2

** merged with CEB in 1998 and renamed "fib"*

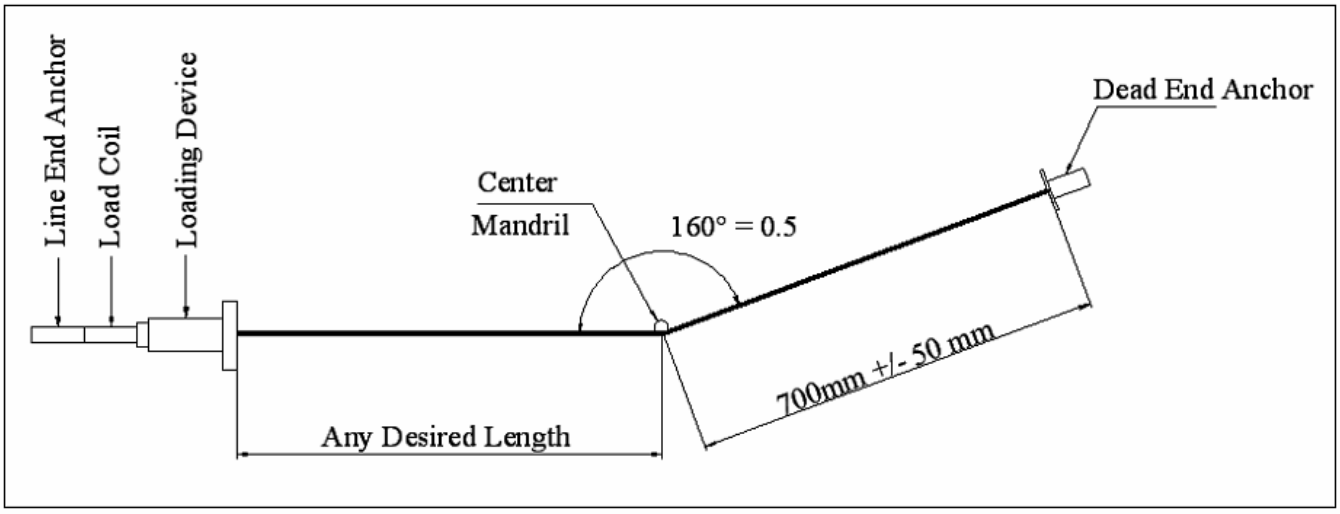

Figure A.1 Detail of One-Pin Test

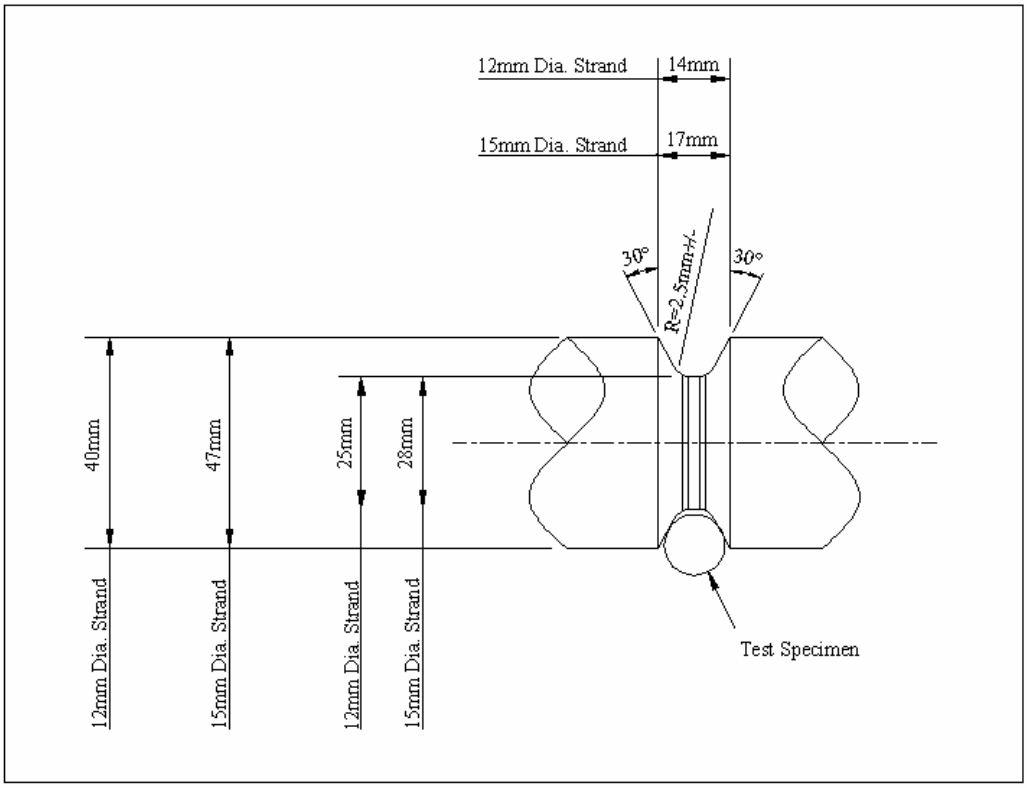

Figure A.2 Detail of Mandril for One-Pin Test

APPENDIX B

TYPICAL MONOSTRAND COMPONENTS WITH DESCRIPTION

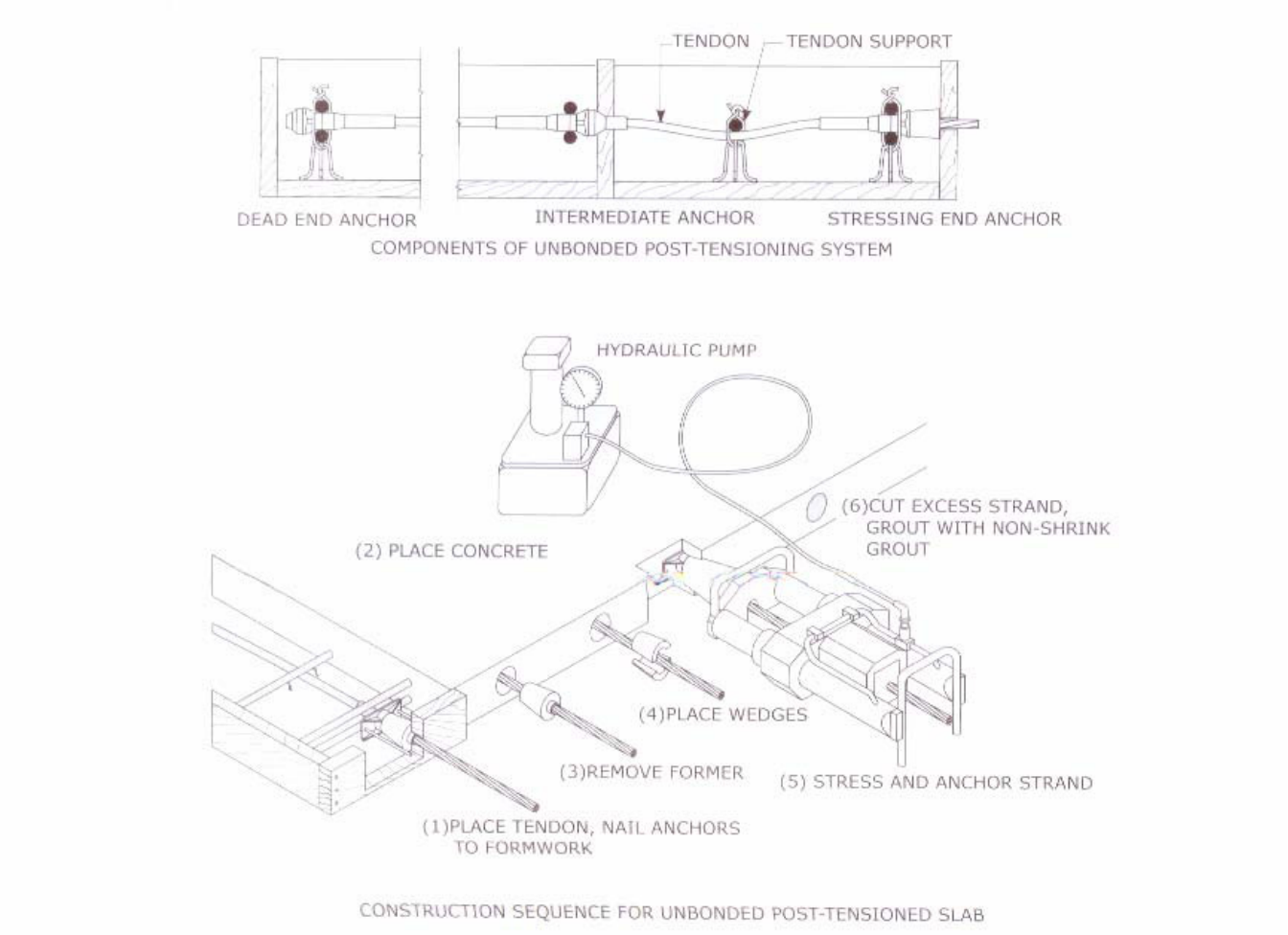

Figure B.1 Components and Construction Sequence for Unbonded Post-Tensioning System (PTI 2006)

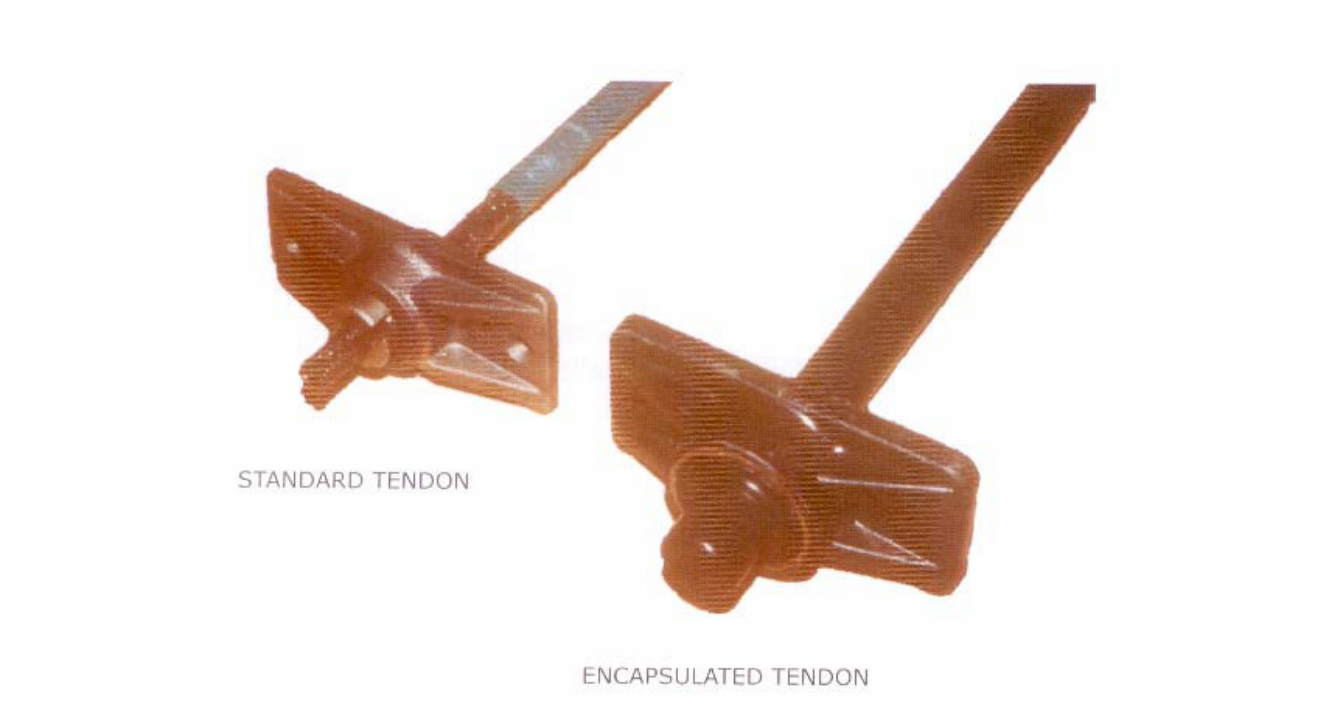

Figure B.2 Standard and Encapsulated Tendon Assembly (PTI 2006)

APPENDIX C

BDII LIVE LOAD ANALYSIS

Table C.1 BDII Live Load Analysis Results (After Mid-Bay (2003))
("Conc" Denotes, for Example, Concurrent Moment with Minimum Shear)

HS20 Truck

Span	Section	Min Shear	Conc Moment	Max Shear	Conc Moment	Conc Shear	Min Moment	Conc Shear	Max Moment
1	1	-191.16	0.00	18.36	0.01	-121.86	-0.04	18.36	0.01
1	2	-184.96	72.09	18.36	-52.74	18.36	-52.74	-25.08	531.71
1	3	-183.89	84.21	18.36	-61.82	18.36	-61.82	-24.95	620.33
1	4	-146.33	1023.66	12.09	1023.66	18.36	-387.70	-62.83	3505.09
1	5	-110.71	2266.19	44.06	2975.04	18.36	-713.58	-26.08	5028.58
1	6	-77.90	3397.11	81.77	4175.93	18.36	-1039.46	-18.62	5502.34
1	7	-48.79	3627.85	117.62	4175.56	18.36	-1365.34	118.28	5097.13
1	8	-24.23	2783.40	150.76	3153.51	18.36	-1691.22	148.64	3860.69
1	9	-5.14	1086.84	180.29	1350.52	18.36	-2017.10	174.73	2017.05
1	10	7.96	-1177.90	205.36	-930.97	18.36	-2342.97	195.66	-95.16
1	11	-4.92	630.30	205.99	-998.29	18.36	-2352.32	-4.92	630.30

Lane Load

Span	Section	Min Shear	Conc Moment	Max Shear	Conc Moment	Conc Shear	Min Moment	Conc Shear	Max Moment
1	1	-207.45	-0.03	21.74	0.01	-176.59	-0.05	17.81	0.01
1	2	-199.32	572.91	21.82	-54.16	24.33	-69.88	-174.17	509.11
1	3	-197.92	667.56	21.85	-61.83	24.33	-81.91	-172.86	594.72
1	4	-151.54	3200.81	36.05	1468.40	24.33	-513.68	-126.56	3133.15
1	5	-111.57	4336.88	59.96	2484.23	24.33	-945.46	-22.51	4687.64
1	6	-78.10	4421.84	88.98	3011.13	24.33	-1377.23	-34.94	5284.20
1	7	-51.06	3797.45	122.45	2827.20	24.33	-1809.00	67.94	4964.35
1	8	-30.28	2788.94	159.54	1771.64	24.33	-2240.77	111.90	3784.98
1	9	-15.41	1692.86	199.28	-243.05	56.24	-2739.15	122.84	1884.35
1	10	-5.99	764.86	240.59	-3218.94	153.80	-4668.54	66.81	710.28
1	11	-5.92	758.20	241.77	-3316.23	156.15	-4746.19	7.53	702.07

Table C.2 Live Load Analysis Results, Adjusted for Impact Factor

Unfactored HS20 Truck

L.L Factor	1.33
Divided by	1.192

Span	Section	Min Shear	Conc Moment	Max Shear	Conc Moment	Conc Shear	Min Moment	Conc Shear	Max Moment
1	1	-213.29	0.00	20.49	0.01	-135.97	-0.04	20.49	0.01
1	2	-206.37	80.44	20.49	-58.85	20.49	-58.85	-27.98	593.27
1	3	-205.18	93.96	20.49	-68.98	20.49	-68.98	-27.84	692.15
1	4	-163.27	1142.17	13.49	1142.17	20.49	-432.58	-70.10	3910.88
1	5	-123.53	2528.55	49.16	3319.47	20.49	-796.19	-29.10	5610.75
1	6	-86.92	3790.40	91.24	4659.38	20.49	-1159.80	-20.78	6139.36
1	7	-54.44	4047.85	131.24	4658.97	20.49	-1523.41	131.97	5687.23
1	8	-27.04	3105.64	168.21	3518.60	20.49	-1887.02	165.85	4307.65
1	9	-5.74	1212.67	201.16	1506.87	20.49	-2250.62	194.96	2250.57
1	10	8.88	-1314.27	229.13	-1038.75	20.49	-2614.22	218.31	-106.18
1	11	-5.49	703.27	229.84	-1113.86	20.49	-2624.65	-5.49	703.27

Unfactored Lane Load

Divided by
1.192

Dead Load Factor			1.00

Span	Section	Min Shear	Conc Moment	Max Shear	Conc Moment	Conc Shear	Min Moment	Conc Shear	Max Moment
1	1	-174.04	-0.03	18.24	0.01	-148.15	-0.04	14.94	0.01
1	2	-167.21	480.63	18.31	-45.44	20.41	-58.62	-146.12	427.11
1	3	-166.04	560.03	18.33	-51.87	20.41	-68.72	-145.02	498.93
1	4	-127.13	2685.24	30.24	1231.88	20.41	-430.94	-106.17	2628.48
1	5	-93.60	3638.32	50.30	2084.09	20.41	-793.17	-18.88	3932.58
1	6	-65.52	3709.60	74.65	2526.12	20.41	-1155.39	-29.31	4433.05
1	7	-42.84	3185.78	102.73	2371.81	20.41	-1517.62	57.00	4164.72
1	8	-25.40	2339.71	133.84	1486.28	20.41	-1879.84	93.88	3175.32
1	9	-12.93	1420.18	167.18	-203.90	47.18	-2297.94	103.05	1580.83
1	10	-5.03	641.66	201.84	-2700.45	129.03	-3916.56	56.05	595.87
1	11	-4.97	636.07	202.83	-2782.07	131.00	-3981.70	6.32	588.98

Table C.3 Live Load Analysis Results, Combined HS20 Truck and Lane Load, 3 Lanes

Combined Live Loads

Number of BD2 Lanes
3

Live Load Factor			1.00
Multiple Presence Factor			0.85

Span	Section	Min Shear	Conc Moment	Max Shear	Conc Moment	Conc Shear	Min Moment	Conc Shear	Max Moment
1	1	-329.23	-0.02	32.92	0.02	-241.50	-0.07	30.11	0.02
1	2	-317.55	476.91	32.97	-88.64	34.76	-99.85	-147.98	867.32
1	3	-315.54	555.89	32.99	-102.72	34.76	-117.04	-146.93	1012.41
1	4	-246.84	3253.30	37.17	2017.94	34.76	-734.00	-149.84	5558.46
1	5	-184.56	5241.84	84.54	4593.02	34.76	-1350.96	-40.79	8111.83
1	6	-129.57	6375.00	141.00	6107.68	34.76	-1967.92	-42.57	8986.55
1	7	-82.68	6148.59	198.87	5976.17	34.76	-2584.87	160.62	8374.16
1	8	-44.57	4628.55	256.75	4254.14	34.76	-3201.83	220.77	6360.52
1	9	-15.86	2237.92	313.09	1107.53	57.52	-3866.28	253.31	3256.69
1	10	3.28	-571.72	366.33	-3178.32	127.09	-5551.16	233.21	416.24
1	11	-8.89	1138.44	367.77	-3311.55	128.76	-5615.40	0.70	1098.42

LIST OF REFERENCES

1. American Association of State Highway and Transportation Officials (AASHTO) (2007). *AASHTO LRFD Bridge Design Specifications*, 4th ed., Washington, DC.

2. American Concrete Institute (ACI) (2005). *Building Code Requirements for Structural Concrete and Commentary (ACI 318-05)*. Farmington Hills, MI.

3. Goni, J. J., and Garcia, A. M. (2009). "Metrorrey's linea 2 extension viaduct: A evolution for light-rail precast concrete segmental bridges." *PCI Journal*, 54(4), 175-188.

4. Mid-Bay Bridge Load Rating (Mid-Bay) (2003). Prepared by Corven Engineering, Inc., Tallahassee, FL, for Florida Department of Transportation (FDOT).

5. Post-Tensioning Institute (PTI) (2006). *Post-Tensioning Manual, Sixth edition*, Phoenix, AZ.

6. Post-Tensioning Institute (PTI) (2004). *Recommendations For Stay Cable Design, Testing And Installation*, 4130 Stay Cable Testing.

7. Specialty Steel (2010). "What Materials and Equipment are Used in Post-Tensioning?" <http://www.specialtysteel.org/PT02.htm> (April 1, 2010).

8. Sumiden Wire Products Corporation (SWPC) (2009). "Effects of Temperature and Bending Stress." <http://www.sumidenwire.com/prod/pc/tech-data/Effects.pdf> (Oct. 1, 2009).

BIOGRAPHICAL SKETCH

H. Houston Spear was born June 11, 1984 in New Port Richie, Florida and has been a Florida resident all his life. He graduated from Archbishop McCarthy High School in Ft. Lauderdale, Florida. He graduated from Florida State University in Tallahassee, Florida with a Bachelor of Science degree in Civil Engineering. His main career focus is in civil engineering, and at the time of this research he is employed by Greenhorne and O'Mara providing engineering inspection services for the Interstate 10 widening project in Leon County. Houston plans to graduate with his Master of Science degree in Civil Engineering and hopes to pursue Professional Engineering and General Contractor licensure in the next few years.